MICROPLASTICS IN MARINE SEDIMENTS OF THE MISSISSIPPI RIVER DELTA (GULF OF MEXICO)

Annerieke Bouwman
MSc - thesis GEO4-1520 (30 ects)
Faculty of Geosciences, Utrecht University
1st supervisor: Prof. Dr. Ir. Caroline Slomp *(Utrecht University)*
2nd supervisor: Dr. Matthias Egger *(The Ocean Cleanup)*

Utrecht University THE OCEAN CLEANUP

Contents

Abstract

The marine environment across the globe is highly polluted with plastics. Plastics have been found at the sea surface, the water column, on beaches and on the seabed. Plastics may persist in the marine environment for hundreds to thousands of years, thus negatively impacting marine organisms.

The current discrepancy between the measured and the modeled size distribution of floating plastic debris reveals a gap in microplastics (<5mm) in the ocean surface waters. The fate of these 'missing plastics' has yet to be unraveled. The seabed has been suggested to be a sink for microplastics. However, data on microplastic accumulation on the seabed remain scarce. Evidence of this accumulation is most likely to be found in areas with large inputs of platics, such as outflows or river which carry plastics collected from land. For this reason, the potential role of the seabed as a sink for microplastics in the Mississippi River Delta (MRD) was studied. Microplastics larger than 30 µm were extracted from surface sediments using a solution of $ZnCl_2$ (1.5 g/cm^3), treated with Fenton's reagent and if necessary with 1M HCl, and analyzed by light microscopy and Raman spectroscopy.

The results show that microplastics were present along the entire depth transect from the mouth of the MRD to the deep sea with concentrations varying between 303 ± 960 and 2705 ± 960 pieces/kg dw (1031 ± 5088 and 18046 ± 5088 pieces/m^2). The highest concentration of microplastics was observed closest to shore. Fibers were the dominant type of microplastics found in all sediment samples, with transparent, yellow and black as the dominant colors. It should be mentioned that fibers had a large input from contamination as well. Hard microplastics ranged from 180 to 643 µm and were identified as high-density polyethylene (HDPE), low-density polyethylene (LDPE), polypropylene (PP), polystyrene (PS), and polyvinylchloride (PVC). Microbeads were identified as PS and polyamide (PA) and their sizes ranged between 245 and 496 µm.

The findings reported in this study indicate that the distribution of microplastics at the river delta is likely controlled by the combination of varying input sources, surface currents, primary productivity and the bathymetry. At the MRD, microplastic concentrations in the seabed are substantially higher than observed at surface waters, the water column and beach sediments. This stresses the importance of the seabed as a sink for microplastics at the MRD.

1. Introduction

Production of commercial plastics started in the 1950s and has since then increased exponentially to a global amount of 330 million tonnes in 2016 (Plastic Europe, 2017). Due to global mismanagement of the plastic waste plastics ends up in the environment (Jambeck et al., 2015). In 2010, between 4.8 and 12.7 million tonnes entered the ocean (Jambeck et al., 2015). As the use of plastic is currently still rising, this number will likely increase by an order of magnitude by 2025 (Jambeck et al., 2015).

Land-based sources of plastics are sewage waters, industries, harbors, cities, unmanaged landfills, littering by beach visitors, illegal dumping and road runoff (Hurley et al., 2018; Veiga et al., 2016; Eriksen et al., 2013). Rivers connect land to the ocean and therefore have a large contribution to the ocean plastic input (Jambeck et al., 2015; Schmidt et al., 2017; Lebreton et al., 2017). Estimates of the yearly riverine input range between 0.4 and 2.75 million tonnes (Lebreton et al., 2017; Schmidt et al., 2017; Schmidt et al., 2018). Ocean-based input comes from fisheries, aquaculture, shipping, offshore activities and recreational boats (Veiga et al. 2016). This input is in the order of 0.1 million tonnes (Shim and Thompson, 2015). A minor source of plastics is the atmospheric fallout of fibers (Dris et al., 2016).

Plastic has been found in all marine systems across the globe, including the sea surface (Law et al., 2010; Cózar et al., 2014), the water column (Kanhai et al., 2018) as well as the seabed (Alomar et al., 2016; Galgani, 1996; Woodall, 2014; Van Cauwenberghe, 2013; Pham, 2014; Fischer, 2015) from the Antarctic to Arctic Oceans. Even the most remote and pristine marine-areas are important sinks for plastics (Boerger et al., 2010; Murray et al., 2011; Alomar et al., 2016; Obbard et al., 2014; Lavers et al., 2015; Peeken et al., 2018; Peng et al., 2018). Plastic items found in the ocean include different types of fishing gear, such as nets, buoys and lines, buckets, bottles, foamed polystyrene, bags, plastic strips, food packages, chairs, supermarket baskets, and plastic fragments (Eriksen et al., 2014; Pham et al., 2014; Galgani et al., 2015; Tubau et al., 2015; Tekman et al., 2017). The size of this plastic debris found in the marine environment range from nanometers to meters (Barnes et al., 2009; Koelmans et al., 2015).

The widespread pollution of plastics and its longevity are a serious problem because its harmful effects on marine life. A wide range of marine organisms is affected by this pollution.

Marine mammals, Turtles, seals, birds and fish may be killed directly due to entanglement in plastic objects such as derelict fishing gear, six-pack rings, bottles and bags (Laist, 1997; Boerger et al., 2010; Dantas et al., 2012) or by clogging of the digestive system due to direct ingestion of plastics (Laist, 1997; Grahams and Thompson, 2009; Foekema et al., 2013; Galloway and Lewis, 2017). Indirectly, toxic chemicals such as polycyclic aromatic hydrocarbons (PAHs), polychlorinated biphenyls (PCBs), polybrominated diphenyl ethers (PBDEs) and nonylphenol (NP) adsorbed to plastics can also harm marine organisms (Teuten et al., 2009; Rochman et al., 2014; Chen et al., 2017; Long et al., 2017). Micro- (< 5mm) and nano- plastics (< 1µm) are thought to be the most harmful to the environment (Eriksen et al. 2014; Blumenröder et al., 2017). These plastics have a similar size as preferred food-items for planktonic filter feeders, and therefore have a higher chance to be ingested (Galloway and Lewis, 2017). Filter feeders are at the base of the marine food web, consumed by predators higher in the food chain. Therefore, ingestion of microplastics by filter feeders forms a high risk of bioaccumulation and biomagnifications.

In addition, smaller plastics sorb more hydrophobic pollutants due to the higher ratio of surface area to volume that increases the sorption capacity (Mato et al., 2001; Martins and Sobral, 2011). Moreover, plankton, fish, seashells, seabirds have been shown to be attracted to plastics with similar colors or odor as their prey (Ryan, 1987; Boerger, 2010; Browne et al., 2008; Savoca et al., 2017). Finally, the plastics and associated contaminants could end up in the human food-chain (Clark et al., 2016).

An experiment of plastic bags covering intertidal sediments showed that it could substantially alter the community structure of infaunal vertebrates and the functioning of the ecosystem (Green et al., 2015). Plastics are not only harmful to the environment; they might be a major carbon source for bacteria and a major diet component of organisms feeding on floating particles > 0.5 mm (Yoshida, 2016; Chen, 2017). So far, this has only been shown at the North Pacific. In addition to acting as a carbon source, large plastics could act as a substrate for epibenthic megafauna or as a shelter for small animals (Katsanevakis et al., 2007; Law, 2017).

Data on the accumulation of plastics in the marine environment is scarce. Existing estimates of the number of plastics residing in Earth's oceans mostly focus on buoyant plastics at the sea surface. The model of Eriksen et al. (2014) shows that at the sea surface, macro plastics (5-50cm) are dominant in weight, whereas microplastics (<5mm) dominate by counts. Most of these small microplastic fragments are the result of the breakdown of larger items (Eriksen et al., 2014).

However, in these estimates small microplastics (20 µm – 1 mm) are underrepresented (Hanke et al., 2013). Eriksen et al. (2014) suggested that there would be a differential loss of small microplastics from surface waters towards the seabed, with numerous biological impacts along the way.

Currently, there is a discrepancy of up to two orders of magnitude between the estimated amount of plastics entering the ocean (4.8-12.7 million tonnes) and the estimated amount of plastics floating at the ocean surface (100s thousands of tonnes) (Eriksen et al., 2014; Van der Wal et al., 2014; Cózar et al., 2014; Jambeck et al., 2015; Matsugumu et al., 2017; Lebreton et al., 2017; Lebreton et al., 2018). Thus, most of the plastics entering the oceans is still unaccounted for. Possible sinks for ocean plastics that are not yet included in global estimates are the water column, the seabed, beaching, ingestion by marine organisms and incorporation into sea ice. Data from these sinks is limited, as plastic accumulation is a relative young research field, possibly due to high sampling costs and restricted methods. Another possibility for the mismatch is that the sampling and analytical methods are not good enough to catch and analyze the tiniest plastic fragments, or models overestimate the riverine inputs.

Plastic will likely persist for hundreds to thousands of years in the marine environment, and even longer in deep-sea sediments due to lower degradation rates of most polymers in the absence of sunlight, and under prevailing low temperatures and oxygen concentrations (Andrady, 2015). Moreover, a quantitative comparison of the plastic abundance in the ocean indicates that the amount of microplastic is two orders of magnitude higher in sediments from the continental shelf than surface waters, and even four orders of magnitude higher in deep-sea sediments than surface water gyres, emphasizing the importance of the seabed as a sink for microplastics (Maes et al., 2017; Woodall, 2014).

In general, ocean plastics are distributed through the ocean by currents, winds, eddies, vertical mixing, deep water cascading events, sea ice and transport processes to the sea floor (Barnes et al., 2009; Yamashita and Tanimura, 2007; Hidalgo-Ruz, 2018; Kukulka et al., 2012; Tubau et al., 2015; Bergmann et al., 2017; Peeken et al., 2018). Marine life plays an important role in this vertical transport of (micro)plastics. First, micro-organisms, crustaceans and invertebrates can colonize the plastics, a process called biofouling (Railkin, 2003; Dobretsov et al., 2010), adding weight to the particles and making them negatively buoyant (Peeken et al., 2018; Andrady, 2011).

Other vertical transfer mechanisms are the transfer via food-webs due to predation of plastic-consuming marine life by animals higher in the food chain (Choy and Drazen, 2013) and the incorporation in animal excretion and fast-sinking (algal) aggregates (Bergmann, 2017; Wright et al., 2013). Microplastics are also transferred downwards in the form of marine snow (Alldredge and Silver, 1988; Porter et al., 2018), resulting from the mixing of water masses with different temperature and salinity which could lead to a density increase (Durrieu de Madron et al., 2005), and by size-selective sinking of fragmented plastic (Lebreton, 2018; Eriksen, 2014, Cózar, 2014; Kooi et al., 2017). The latter transfer mechanism is the current consensus based on the missing size-fraction < 2.2 mm in ocean surface waters. These small fragments are removed in large amounts by size-selective sinks such as ingestion by marine organisms, nano-fragmentation processes and biofouling (Wright et al., 2013; Cózar et al., 2014; Kooi et al., 2017). This supports the hypothesis of substantial losses of plastics from the ocean surface waters. Plastics from deep waters can return back to the surface or intermediate depth as a result of defouling (Cózar et al., 2014; Kooi et al., 2017). This process occurs when conditions are unfavorable for epiphytic organisms to live or when carbonated and opal dissolute due to acidic conditions (Cózar et al., 2014).

In spite of various studies on the transport mechanisms of plastics to the ocean floor as well as the breakdown of plastics, the topics are not well understood. There is a need for improving our understanding of these mechanisms as that will contribute to the important debate on microplastic distribution in the marine environment and what its accompanying impacts are. The seabed likely acts as an important sink for plastics in the marine environment and therefore is a crucial topic to study. It is difficult to get these samples as it requires a suitable well-equipped a ship and it is expensive. Galgani et al. (1996) reported the accumulation of debris, including plastics, at the Mediterranean seafloor. Van Cauwenberge et al. (2013) was the first to show the presence of microplastic in deep-sea sediments of the South Atlantic Ocean (2479-4881 m water depths), the Porcupine abyssal plain in the North Atlantic (4842-4844 m) and in sediments of the Congo canyon (4785 m water depth), with sizes of microplastics ranging from 76-161 µm. Woodall et al. (2014) revealed the presence of microplastics in marine sediments at several locations across the Mediterranean (300-3500 m), the North Atlantic (1000-2000 m) and the Southwest Indian Ocean (500-1000m) with an average size of 2-3 mm. Microplastics have also been observed at the Kuril-Kamchatka trench and Mariana Trench at a depth between 4869-5766 m, 300-10908m respectively (Fischer, 2015; Peng et al, 2018).

The presence of microplastics has been more often reported in coastal and beach sediment in both highly populated areas and remote areas compared to the deep-sea (Kusui and Noda, 2003; McDermid and McMullen, 2004; Turner and Holmes, 2011; Martins and Sobral, 2011; Browne et al., 2011; Liebezeit and Dubaish, 2012; Turra et al., 2013; Alomar et al., 2016; Bergman et al., 2017; Lavers et al., 2017; Hidalgo-Ruz et al., 2018; Zhou et al., 2018).

Several sampling, extraction and analytical methods have been used to obtain and identify microplastics in marine sediments. As a result, the data is difficult to compare. First of all, marine sediments are sampled as a surface area or as a bulk sample, reporting abundances in pieces per surface area and pieces per weight or volume, respectively (Van Cauwenberghe et al., 2015). Due to missing reported information such as the sampled sediment depth, conversion between the two units is not always possible (Van Cauwenberghe et al., 2015), hindering the comparison of different studies. In the laboratory, the most common method to extract plastics is by a density separation method (Löder and Gerdts, 2015; Hidalgo-Ruz et al., 2018), where the plastics will float on top of the added liquid. Used liquids vary in density from 1 to 1.8 g/cm^3 (Löder and Gerdts, 2015; Hidalgo-Ruz, 2018), resulting in different extraction efficiencies as the density of plastics ranges from 0.89 to 1.7 g/cm^3 (US EPA,1992). For this density separation, glass beakers (Woodall et al., 2014), a so-called Munich Plastic Sediment Separator (Imhof et al., 2012) or the Sediment-Microplastic-Isolation (SMI) unit (Coppock et al., 2017) have been used. Microplastics have also been extracted by elutriation and flotation (Claessens et al., 2013), as well as by an oil extraction method (Crichton et al., 2017).

Extracted microplastics are identified by visual analysis (Woodall, 2014; Fischer, 2015; Blumenröder, 2017; Vianello, 2013; Maes, 2017) and subsequently categorized according to their size, shape, color and weathering morphologies (Nor and Obbard, 2014; Löder and Gerdts, 2015). Identification based on or coupled with more accurate methods such as Raman spectroscopy (Cauwenberge 2013), Fourier Transform Infrared Spectroscopy (FT-IR) and Pyrolysis Gas Chromatography coupled to Mass spectrometry are more reliable (Jambeck et al., 2015; Lavers et al., 2017; Maes et al., 2017; Nor and Obbard 2006; Nor and Obbard, 2014; Fischer and Scholz-Böttcher, 2017).

In this project, sediment samples collected from the Mississippi River Delta (MRD, - Gulf of Mexico) are investigated for microplastics. River deltas are important to study as they likely retain a lot of plastics. Stations are located in a transect from the MRD towards the open ocean. Samples were taken with a multi-corer.

Then, the microplastics were extracted from the sediment by density separation with a $ZnCl_2$ solution (1.5 g/cm^3), followed by the removal of organic material with Fenton's reagent and if necessary subsequent decalcification with 1M HCl. Extracted microplastics were subsequently characterized by visual analysis with a light microscope and with Raman spectroscopy. Microplastics have been found along the entire depth transect in concentrations between 300 and 2700 pieces/kg dw (5156 and 90230 pieces/m^2), with a dominance of fibers. Hard plastic particles were identified as PE, PP, PS and PVC and microplastic beads as PS and PA. The results from this research provide new insights into the role of the seabed as a sink for marine plastic debris. Such information is urgently needed to close the ocean plastic mass balance.

2. Materials and methods

2.1 Study site and sampling

The Gulf of Mexico is a semi-enclosed basin. The Mississippi-Atchafalaya river basin has a size of about 3.4 million km^2, draining 40% of continental US and is the third largest in the world (NPS, 2017; Broussard, 2007; EPA, 2018). The length of the Mississippi River from the source Lake Itasca to the Gulf of Mexico is about 3800 km (NPS, 2017), with a water discharge between 7000 and 20.000 m^3/s (Syed et al, 2005). The Atchafalaya River, with a length of 225 km, is the main distributary of the Mississippi River and merges into the Gulf of Mexico (Richard, 2016). The Mississippi river belongs to the top 14 most plastic polluted rivers in the world (Lebreton et al., 2017). The Mississippi basin is highly populated, around 71 million inhabitants (US Census, 2016) and industrialized. Urban waste and packaging material from the industrial sector are both sources of riverine plastics (Van der Wal et al. 2015). About 7000 wastewater treatment plants are located in the catchment area (Bluetech, 2014), which have been shown to be an import source of riverine plastics (Browne et al., 2011; Van der Wal et al., 2015; Vermair et al., 2017). With 57% of the US farmland located within the Mississippi basin, agricultural activities act as a source of pollution as well. Other sources are fisheries and medical waste (Van der Wal et al., 2015). All material that has entered the watershed can potentially discharge into the Gulf of Mexico and possibly end up at the sea floor.

Sediments samples were collected with a multicorer (10 cm diameter, 10 cm depth) during the Netherlands Initiative of Changing Oceans (NICO) expedition leg 7 (12.3-4.4.2018) at six locations along a transect from the MRD towards the open ocean (16 mbss, 53 mbss, 130 mbss, 288 mbss, 546 mbss and 2100 mbss, respectively) (Fig. 1, Table 1). The top 5 cm of each core was sliced under oxic conditions and was immediately transferred into aluminum bags and thoroughly sealed to prevent contamination. Samples were subsequently stored at -20 ^{0}C (NICO 7 cruise report, 2018).

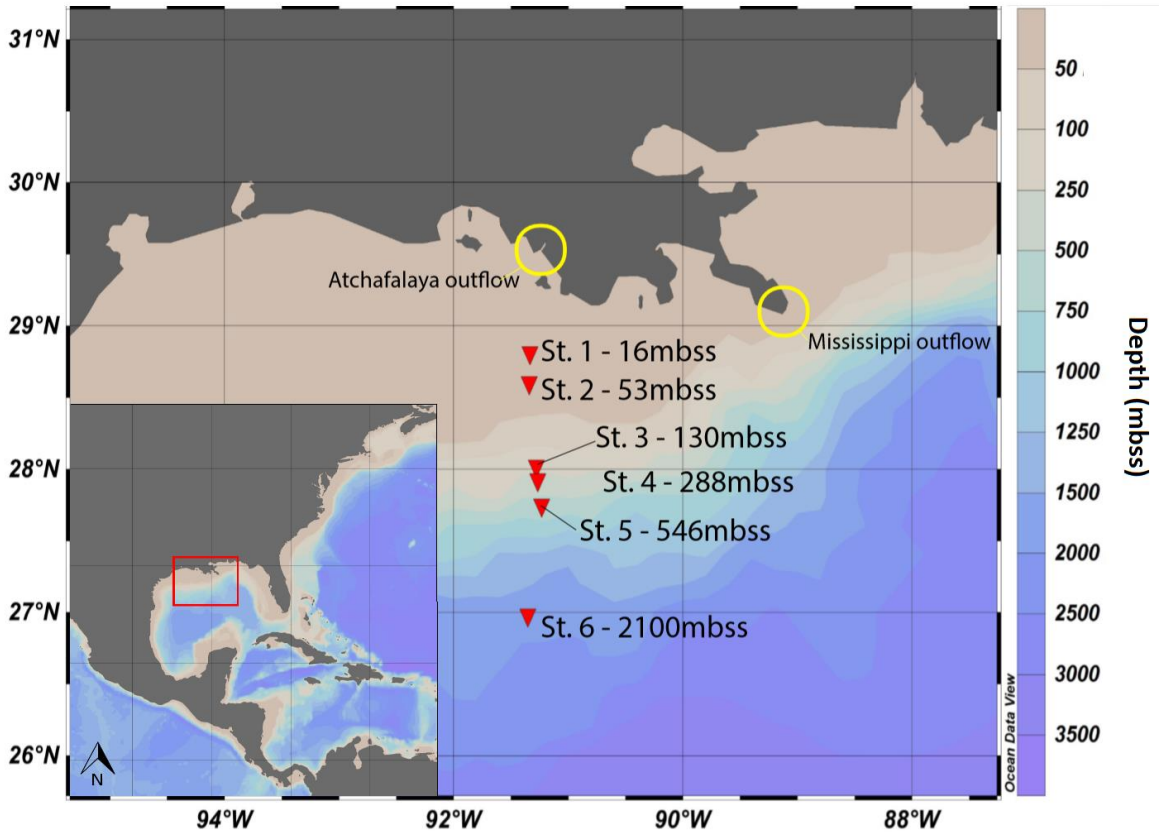

Figure 1. The locations of the six sampling sites in front of the Mississippi River Delta (MRD) and corresponding water depths in meters below sea surface (mbss) (adapted from Van Zummeren, 2018).

Table 1. Depth and coordinates of the six sampling stations.

Station	Depth (m)	Location (latitude, longitude)
1	16	N 28° 48' 5.767" W 91° 20' 1.262"
2	53	N 28° 26' 6.346" W 91° 20' 20.587"
3	130	N 28° 0' 40.054" W 91° 16' 38.042"
4	288	N 27° 54' 53.802" W 91° 15' 55.681"
5	546	N 27° 44' 21.106" W 91° 13' 51.755"
6	2100	N 26° 58' 21.731" W 91° 21' 2.776"

2.2 Microplastic extraction and characterization

In the lab, sediments were dried for 92 h in an oven at 60^{o} until completely dry. Subsequently, microplastic particles were extracted by density separation using the Sediment Microplastic Isolation (SMI) unit developed by Coppock et al. (2017) and a $ZnCl_2$ solution of 1.5 g/cm^3. To obtain 500mL of this solution, 350 g of $ZnCl_2$ (s) was added to 370 ml of Milli-Q water. The SMI-unit consists of three pieces, a lower and upper column with a ball valve in between. This ball valve has the capacity to close the lower column from the upper column. Both columns and the stability plate of the SMI are made from polyvinylchloride (PVC), a plastic type that is resistant to corrosion (Coppock et al., 2017). The ball-valve is made from both PVC and polyethylene (PE). The SMI-unit is easy to construct has reduced costs and is durable and light in weight (Coppock et al., 2017). Moreover, Coppock et al. (2017) showed that the recovery rate of the unit is 95%. Together with the fact that the unit is easy in use and has low costs, it was shown to be a reliable method to extract plastics from different types of marine sediments. The downside is that the SMI unit has not been tested for long term use. Continuous use of $ZnCl_2$ can result in the degradation of the SMI unit and therefore potential contamination of PVC and HDPE (Coppock et al., 2018).

By using a solution with a density of 1.5 g/cm^3, plastic particles of the following polymer types were able to float onto the solution: high-density polyethylene (HDPE), low-density polyethylene (LDPE), polypropylene (PP), polyvinylchloride (PVC), polyethylene terephthalate (PET), polystyrene (PS), expanded polystyrene (EPS), polyamide (PA), polycarbonate (PC), polymethylmethacrylate (PMMA), acrylonitrile/butadiene/styrene (ABS), polyurethane (PUR), polytetrafluoroethylene (PTFE) (Table 2). PTFE has a higher density than the used $ZnCl_2$ solution and can therefore not be extracted with this method. PA and ABS with additives and PTFE can have a higher density than the used $ZnCl_2$ solution, and so a fraction of these polymers might not be extracted (Table 2). With the use of this solution, sediments consisting of minerals like quartz, potassium, feldspar, light mica, magnetite and calcite, will settle (Table 2).

Table 2.. Density of polymer types, polymer types with additives and minerals (adapted from Nuelle et al., 2014

Polymer abbr.	**Polymer name**	**Density (g/cm^3)**	**Density with additives (g/cm^3)**	**Mineral**	**Density (g/cm^3)**
HDPE	High-density polyethylene	0.94-0.97	1.18-1.28 (PE)	Quartz	2.65
LDPE	Low-density polyethylene	0.89-0.94	1.04-1.17	Potassium Feldspar	2.56
				Light Mica	2.80
PP	Polypropylene	0.89-0.91			
			1.3-1.7	Magnetite	5.2
PVC	Polyvinylchloride	1.3-1.58			
				Calcite	2.7
PET	Polyethylene terephthalate	1.29-1.40			
PS	Polystyrene	1.04-1.08	1.2-1.5		
EPS	Expanded polystyrene	0.015-0.03			
PA	Polyamide	1.07-1.08	1.13-1.62		
PC	Polycarbonate	1.20			
PMMA (acrylic)	Polymethyl-methacrylate	1.17-1.20			
SAN	Styrolacrylnitrile	1.02-1.08			
ABS	Acrylonitrile/butadiene /styrene	1.01-1.08	1.18-1.61		
PUR	Polyurethane	1.17-1.28			
PTFE	Polytetrafluoroethylene	2.14-2.2			

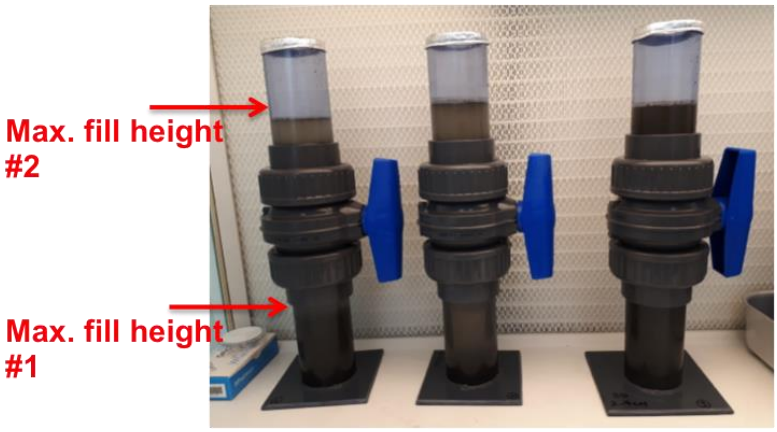

***F**igure 2. Sediment Microplastic Isolation (SMI) unit used for the density separation. $ZnCl_2$ is added to max. fill height 1, before sediment is brought into suspension, and to max. fill height 2 before settlement of the sediment.*

Before the assembly of the SMI unit, each component was thoroughly rinsed with Milli-Q water. Next, a filtered (21 µm filter size) $ZnCl_2$ solution (1.5 g/cm^3) was put into the SMI-unit until 2 cm above the ball valve. The ball valve was opened and closed a few times to fill the cavities of the ball valve with the $ZnCl_2$ solution. Subsequently, $ZnCl_2$ solution was added to the SMI-unit with closed valve up to 5 cm below the top (Fig. 2). The unit was left for about 10 minutes to allow contaminants to float to the surface. Then, the ball valve was set in an open position and the solution was filtered over a 10 µm metal or a 21 µm polycarbonate filter by using a vacuum filtration apparatus. Again, the ball valve was opened and closed a few times to remove the $ZnCl_2$ from the cavities, and filtered as well. The process was repeated until no contaminants (white and transparent fragments and fibers) were visible on the filter under the light microscope and each SMI-unit was free of contaminants. Before each new extraction, this process was performed twice and the filters were visually inspected by eye for contaminants. Metal filters appeared not to be suitable for the extraction of microplastics, therefore polycarbonate filters (21 µm) were used for filtering the solutions and nylon filters (30 µm) for the extractions.

When the SMI-units were prepared for extraction, about 25 g of dry sediment was added to each unit. First, the sediment was loosened using a clean agate mortar in the fume hood, making sure not to grind the sample. The $ZnCl_2$ solution was added halfway of the lower column (max. fill height #1, Fig. 2), afterward the unit was moved in a circular motion to get all the sediment in suspension. Then, the units were filled until 5 cm above to valve with $ZnCl_2$. To make sure no air remained in the ball valve; the valve was opened and closed carefully a few times.

Subsequently, the units were filled with $ZnCl_2$ until 5 cm below the top (max. fill height #2, Fig. 2), and the solution was mixed with a stirring bar on a stirring plate for approximately 2 h. Subsequently, the sediment was let to settle overnight. The next day, the solution in each upper chamber was filtered through a 30µm nylon filter (47 mm diameter) by using a vacuum filtration apparatus. To obtain all particles, the upper chamber was rinsed a few times with $ZnCl_2$ solution until no particles were visible and filtered over the nylon filter. The extraction of the particles was performed in the fumehood with inward laminar flow.

After each extraction, the SMI- units were cleaned. First, the whole unit was rinsed with first demi-water and then with Milli-Q water. Then, the unit was disassembled, and each compartment was rinsed with Milli-Q water. Special attention was given to the ball valve, as sediment could accumulate in the cavities of the valve. After assembly, the SMI-unit was cleaned once more with Milli-Q water. Before the next extraction, potential contaminants were removed by adding $ZnlCl_2$ solution, as described before.

$ZnCl_2$ is highly toxic for aquatic life and human (Toxnet, 2018), therefore it is re-used. To be able to re-use the $ZnCl_2$, sediments and contaminant particles had to be removed first and the density of the solution was checked. First, sediments were able to settle overnight, after which the solution was decanted and underwent sequential filtration (200 µm, 100 µm, 55 µm, 30 µm, 21 µm). The solution was filtered three times over the 21µm filter to remove contaminant particles. To check the density of the solution, 100 mL of $ZnCl_2$ was added to a clean glass-cylinder and weighed. When the density dropped below 1.4 g/cm^3, $ZnCl_2$ (g) was added until the solution had a density of 1.5 g/cm^3.

Prior to Raman spectroscopy, the filters with the extracted material were treated with Fenton's reagent to remove the organic material covering the particles (adapted from Bergmann et al. (2017) and Hurley et al (2018)). This removal reduces the fluorescence of organic matter with Raman spectroscopy. For this reagent, 1 g of $FeSO_4$ was added to 50 ml of Milli-Q water, and the pH was adjusted to 3 with concentrated sulphuric acid (H_3SO_4). Filters were placed in a clean 250 ml glass beaker and 10 ml of $FeSO_4$ solution was added, followed by slow addition of 20 ml of H_20_2 (30%). During this step, the glass beaker was placed in a water bath (20 ^{O}C) because of the exothermic reaction. After 15 minutes, the filter was rinsed with Milli-Q water above the beaker and the solution was filtered back over the same filter. This process was performed in a fumehood with a laminar inward flow as well.

Table 3. Methods used for visual analysis for each sample, the fraction of the samples lost during the visual analysis and the total weight of the sediments.

Station	Method 1 (%)	Method 2 (%)	Method 3 (%)	Lost (%)	Total (g)
1	0	19	42	29	263
2	35	0	65	0	143
3	0	21	79	0	237
4	42	0	58	0	120
5	30	0	70	0	167
6	28	0	63	0	134

After the removal of organic matter, the filters were analyzed using a light microscope (Leica Si9) with an amplification between 30 to 40, depending on the size of the particles. The initially defined protocol of the visual analysis was not suitable for this research. Therefore, the methodology has been improved during the research period. As a result, three different methodologies have been used. First, all potential plastics were collected on a metal filter with a mesh size of 10 µm in a clean glass petri dish (diameter of 47 mm). Unfortunately, the petri dish with collected particles from 29% of the analyzed sediment sample of Station 1 flipped on top of the table and all particles were lost (Table 3). Therefore, the method was adjusted to prevent the loss of data. In the second method, each type of potential microplastic particles was photographed once and collected on a metal filter and similar appearing particles were noted. First, particles were placed randomly on the filter, but later the particles were placed systematically on the metal filter to be able to find all particles back easily during Raman analysis. However, as particles moved over the filter and were difficult to find back, the method was further improved. All picked particles were systematically placed on a cardboard (made out of cardboard, glass slice and a metal holder). No loss of particles is possible from this cardboard and all particles could be found back under the Raman microscope. Table 3 shows which method was used for which sample. During method 2 and 3, the number of particles lost when transferring the particles with a tweezer from the sample to the filter or cardboard was noted as well.

During the visual analysis, only potential microplastic particles were collected for Raman analysis. Fibers were characterized by color, and for each sample, the number of fibers per color was noted.

The distinction in the characterization of the microplastic particles and fibers was made to reduce the time for microplastic identification as all samples contained a high amount of fibers. In addition, it was expected that fibers would be a major source of contamination.

The collection of potential microplastic particles is based on the criteria defined by Cole et al. (2011), Norén et al. (2017), and Nor and Obbard (2014): 1. No cellular or organic structures visible, 2: colored particles are homogeneously colored, 3: particles are not shiny, 4: fibers are equally thick throughout the entire length and not tapered at the end, 5. fibers are not segmented or appear twisted flat ribbons.

The high calcareous content of samples from 546 mbss hampered the visual analysis under the microscope. Therefore, these filters were decalcified. Before this decalcification, the filter was quickly scanned under the microscope for microplastics. Fibers were already noted. For the decalcification, filters were placed into a 250 ml clean beaker glass. Then, 1M HCl was added in steps of 2.5 mL until the filter was fully submerged and an addition did not result in a chemical reaction. No more HCl was added if an addition did not result in a reaction. When the reaction was finished, the filter was rinsed with Milli-Q water above the beaker on both sides until a visual inspection showed that no particles were attached to it. Then, the solution was filtered back onto the same filter. The beaker was rinsed for a few times to make sure all particles were transferred to the filter. The filtration unit was also rinsed with Milli-Q water to make sure no particles got stuck to the unit. The filter was placed back into the glass-petri dish. After drying the filters at room temperature in the closed petri-dish, they were re-examined under the microscope.

HCl (>20%) has been shown to degrade several types of plastic polymers (Nuelle et al., 2014). To test the resistance of various polymers to 1M of HCl, and the potential loss of plastic by the decalcification, the following polymers were exposed for 15 minutes to 1M HCl: HDPE, LDPE, PP, PS, PA, nylon, PET, PVC, PTFE. Of every polymer type, 5 particles of size 4-6 mm and 10 particles of 1-3 mm were added to the solution. Those particles were obtained by cutting collected material made from a specific polymer type into smaller pieces (Table 4). Before and after the experiment, the particles were weighted all together in a glass petri dish on a balance with an accuracy of three decimals and visually inspected with a light microscope to notify if degradation did occur.

Table 4. Used material for the most abundant polymer types as Raman references.

Polymer type	Used material as Raman reference
HDPE	lab equipment bottle
LDPE	ANWB plastic back
PP	package oral-b dental floss
PA	lab material, ring to prevent for corrosion
cellulose acetate	cigar filter
PS	disposable cup
PVC	water hose
PET	package AH "Tijd voor ontbijt Walnoten & jumbo rozijnen"
Nylon	fishing wire
PTFE	

Collected potential microplastic particles were characterized by using Raman spectroscopy (red laser, wavelength 785 nm). Besides, the size of the particle was noted. To be able to identify particles, a Raman library of the most commonly found plastic polymer types has been created: HDPE, LDPE, PP, PS, PA, PET, cellulose acetate and nylon (Table 4). The spectra of each particle were compared with this library (Attachment 1). For this analysis, the software of WITEC project 4 has been used. If not fit with the reference spectra was found, the particle was identified by visual comparison of the findings with other studies.

2.3 Contamination control

To prevent for contamination in the laboratory, a white cotton lab-coat and nylon gloves were worn, the experiments were performed in a fume hood with an inward laminar flow. In addition, exposure of the samples to air was minimized, all lab-equipment was rinsed three times with Milli-Q water before usage and squeeze bottles were rinsed with Milli-Q until potential contaminants were removed. The latter was checked by filtering the solution over a 21 µm polycarbonate filter and visual inspection under a light microscope. To prevent for cross-contamination of the samples, the equipment was rinsed three times with Milli-Q water in between, and the agatar was rinsed with ethanol as well.

During each process step, contamination was controlled. First, the contamination by the SMI-unit was tested. A total of eight blanks were performed, were only $ZnCl_2$ was added to the SMI-unit.

This blank underwent the same process as the samples, including the treatment with the Fenton's reagent. Additionally, after three extractions were performed the SMI-units were examined for degradation both visually and by blanks. These procedural blanks were carried out because the long-term use of the units has not been tested yet (Coppock et al., 2017). The contamination in the fumehood was controlled by placing a 21 µm polycarbonate filter (47 mm diameter) in an open glass petri-dish when the samples were exposed to the air in the fumehood. During each extraction round and subsequent treatment with Fenton's reagent, a new filter was placed in the fumehood. During one extraction round, sediments from one to two stations were processed. Therefore, the contamination during one extraction round cannot be linked to a specific station.

To make sure the solution of $ZnCl_2$ was not contaminated with potential plastics and could be reused, the 21 µm polycarbonate filter was visually inspected. If necessary, the solution was re-filtered over the 21 µm polycarbonate filter until the solution was free of contaminants.

During the visual analysis, the samples were exposed for a minimal period of time to the air.

Table 5. Sources of potential contaminants during the extraction and characterization of the microplastics, their polymer type and color.

Polymer type	**Color**	**source of contamination**
LDPE	Transparent	squeeze bottle used for Milli-Q water and $ZnCl_2$ solution
PVC	transparent, blue, grey	SMI-unit, a tube attached to filtration erlenmeyer flask
PE	white	valve of SMI
HDPE	black	H_2O_2 (s) bottle
HDPE	White	bottles of $ZnCl_2$ (s) and $FeSO_4$ (s), and material from the ball valve
nylon	transparent	filter 30 µm
polycarbonate	transparent	filter 21 µm
	transparent	pipets
	white,	coating magnetic stir
diverse fibers	diverse	air in fumehood and microscopy room
diverse fibers	diverse	milli-Q water

To reduce for potential contamination, the microscope and the table top were cleaned with a paper towel before opening the glass petri-dish with the samples. To obtain the average contamination over the entire period a 21 µm polycarbonate filter in an open glass-petri dish (47 mm diameter) was placed on the table during the entire period of visual analysis. The petri-dish was closed when no sample was exposed to the air. To obtain the contamination for every single sample, a distinction was made between fibers in the sample and the ones lying on top of the sample during the counting and characterization of the fibers by color. The latter was assumed to be contamination. Each filter of the contamination control was analyzed visually and by Raman spectrometry, as described for the samples.

Table 5 shows the polymer-type of each lab-equipment used during the extraction and characterization process. Each of them could potentially have contaminated the samples.

2.4 Classification of microplastics

In this study, microplastic particles were classified based on the classification of Laurent et al. (2018), containing the following four groups: 'H' type - fragments and objects made out of hard plastics, plastic sheet or film, 'N' type - plastic lines, ropes and fishing nets, 'P' type – pre-production plastic pellets in the shape of a cylinder, disk or sphere, and 'F' type – fragments or objects made of foamed material. The study of Lebreton et al. (2018) focused on buoyant plastics in the ocean surface. Here, we add two additional classes for microplastics in sediments, 'Fb'- fibers and 'B' micros - spheres from cosmetics and soaps.

2.5 Units used to express microplastic concentrations

In microplastic research, concentrations of microplastics are expressed in pieces per surface area, pieces per weight and pieces per volume. To be able to compare our results to different studies, units are expressed in both pieces/kg dw and pieces/m^2. First, the amount of counted microplastic particles found per station and type of contamination were normalized to the amount per kilogram dry weight (pieces/kg dw). For the blanks, the number of microplastics were normalized to 25 g of sediment, a similar weight as used during a single extraction. For the contamination in the fumehood, the number of counted microplastic is corrected for the total amount of sediment processed during that specific extraction round. The contamination during the visual analysis is corrected per sample site, therefore also the total sediment weight of the sample site. Then, the concentration in pieces/kg dw was converted to pieces/m^2 for a depth interval of 1 cm according to Equation 1.

$$MPs, surface = \frac{MPs, weight * SED}{S * d} \qquad \textit{Equation 1}$$

MPs,surface = concentration of microplastics for a depth interval of 1 cm (pieces/m^2)

MPs,weight = concentration of microplastics (pieces/kg dw)

SED = total dry sediment weight of the sample (Table 3) (kg)

S = surface area of the multicorer = 79E-4 (m^2)

d = sample depth = 5 (cm)

The conversion from pieces/kg dw to pieces/m^2 for the contamination controls is done according to Equation 2, assuming a sediment density of 2.65 g/cm^3. This conversion equation has also been applied to convert reported microplastic concentrations of other studies in pieces/kg dw to pieces/m^2 and the other way around (Tables 9, 11 and 13). For these studies, the given microplastic concentration is for a depth interval of 1 cm.

$$MPs, surface = \frac{MPs, weight * D * p}{d} \qquad \textit{Equation 2}$$

D = average sediment density of 2.65E-3 (kg/cm^3)

p = a conversion factor to convert cm^2 to m^2 = 10000 (cm^2/m^2)

d = sample depth (cm)

2.6 Statistical analysis

Microplastics were lost when transferring them with a tweezer from the sample to the filter or cardboard. Both, the total number of transferred microplastics and the number of lost microplastics were noted. For each sample, the fraction of lost particles was calculated according to Equation 3.

$$P, loss, i = \frac{P, total, i + P, lost, i}{P, lost, i} * 100\% \qquad \textit{Equation 3}$$

P,loss,*i* = the percentage of lost microplastics during the transfer of the particles during the visual analysis, analysis for sample *i*. (%)

P,total,*i* = total amount of successfully transferred microplastics during the visual analysis for sample *i* (-)

P,lost,*i* = total amount microplastics lost during the transfer during the visual analysis for sample *i.* (-)

Each single blank and fumehood control cannot be associated with a single station, therefore the average and standard deviation of the contamination by the eight blanks and the six fumehood controls was calculated. The total amount of contamination per station is the sum of the contamination of the blank, of the fumehood and of the contamination during visual analysis of the particular station.

The characterized fibers were corrected by the identified fibers of every single source of contamination. For this correction, the average amount of contamination of the blank and fumehood was used and subtracted from the amount of counted fibers (Eq. 4). The correction has been made for every single color (Eq.4).

$$Fbcorr, i, s = Ftot, i, s - Fb, i - Ff, i - Fv, i, s \qquad \textit{Equation 4}$$

Fcorr,*i*,*s* = fiber concentration (pieces/ kg dw) corrected for contamination for color *i* at station *s;*

i is a single color or the sum of all these color;

s is the station number: 1,2,3,4,5 or 6, or the sum of all stations.

Ftot,*i*,*s* = total concentration of counted fibers (pieces/ kg dw) of color *i* at station *s*

Fb,*i* = average concentration of fiber contamination (pieces/ kg dw) by the blank for color *i;*

Ff,*i*= average concentration (pieces/ kg dw) of fiber contamination in the fumehood for color *i*;

Fv,*i*,*s*= concentration of fiber contamination during visual analysis (pieces/ kg dw) of color *i* at station *s*.

3. Results

The results are expressed in both pieces/kg dw as pieces/m^2. The latter is put between brackets. Both units will show a slightly different trend of the microplastic concentration along the depth transect. This is the result of the variable porosity of the sediments at each station (Table 6), which is included in the expression of microplastic concentrations in pieces/m^2 but excluded when expressed in pieces/kg dw. Here, the results are discussed for microplastic concentrations in pieces/kg dw.

3.1 Microplastic distribution along the depth transect

Microplastics are present along the entire depth transect (Fig. 3a), with the highest concentration of 4592 pieces/kg dw (30633 pieces/m^2) found at Station 1. With increasing distance from the coast, the concentrations decrease to 2141 pieces/ kg dw (12861 pieces/m^2) at Station 3, increases again at Stations 4 and 5 (2769 and 3178 pieces /kg dw; 8430 and 13468 pieces/m^2) and finally decrease again at Station 6 (2127 pieces/kg dw; 7241 pieces/m^2). Microplastics of types N, P and F have not been found. Fibers are by far the most abundant microplastics. Hard plastics and microbeads are found as well, but in concentrations that are a factor 100 to 1000 times lower than those for fibers. Hard plastics are present at each station except Station 5, with concentrations between 4 and 133 pieces/ kg dw (25 and 405 pieces/m^2) (Figs. 3 and 4a). The amount is highest at Station 4. Microbeads have been found at Stations 2, 4, 5 and 6, with concentrations varying between 14 and 74 pieces/kg dw (51 and 253 pieces/m^2), and with the highest concentrations at Station 6 (Figs. 3 and 4b).

Table 6. The average porosity for the top 4.75 cm of the sediments for the six stations. Data received from Van Helmond (2018, Geochemistry group, Utrecht University.)

	St. 1	**St. 2**	**St. 3**	**St. 4**	**St. 5**	**St. 6**
Porosity (%)	80.74	86.74	88.67	81.82	90.3	90.1

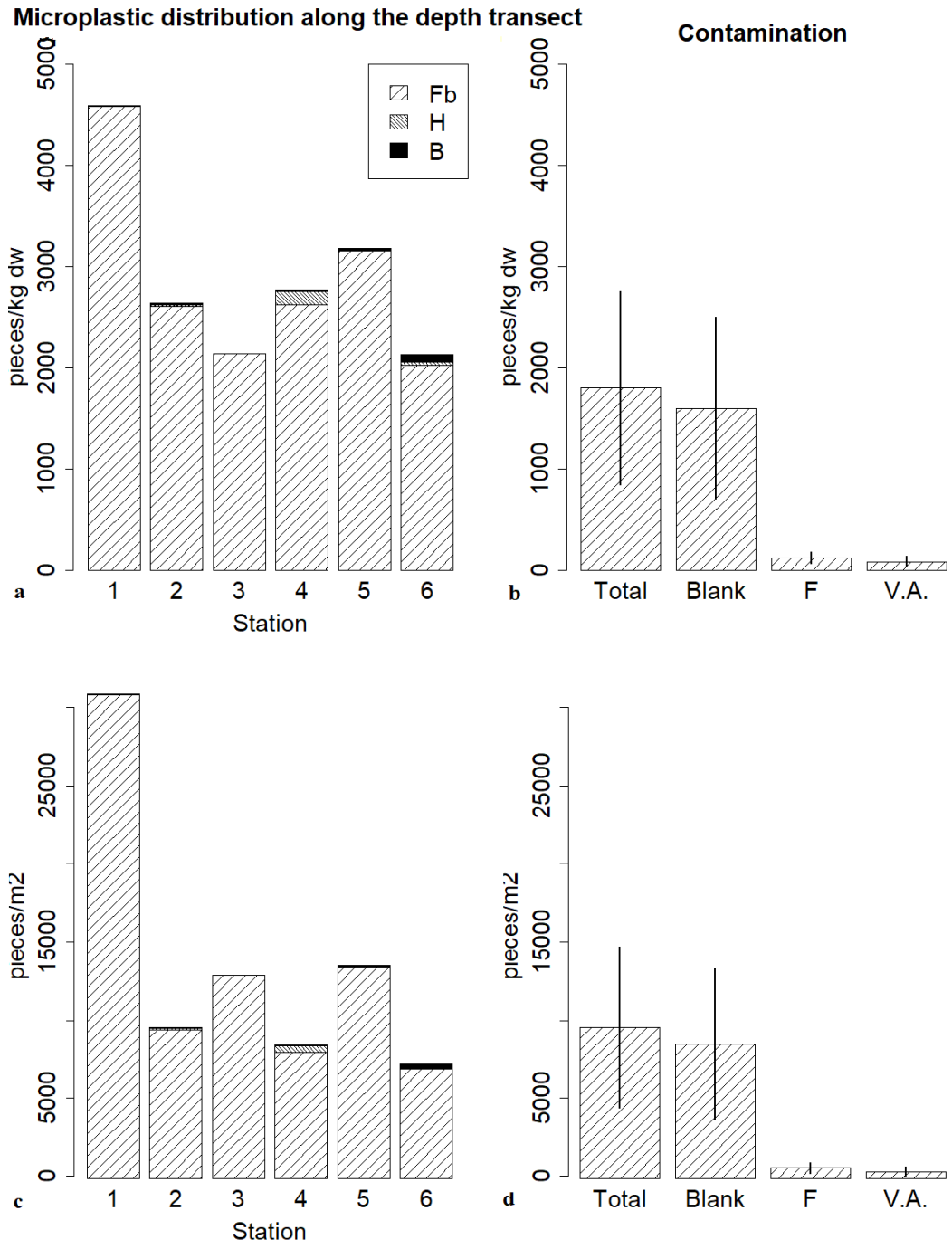

Fig. 3. a, c) Microplastic distribution along the depth transect; fibers, fragments and microbeads in a) pieces/kg dw, c) in pieces/m^2, b,d) The amount of contamination in the blank, the fumehood (F), the during visual analysis (V.A.) and the sum of the blank, F and V.A b) in pieces/kg dw, d) in pieces/m^2. Bars indicate the average amount of contamination and the error bar the variation (standard deviation) in contamination. Contamination in F and during V.A. was only by fibers, whereas blanks had next to fibers also minor contamination by hard plastics (10 ± 17 pieces/kg dw = 53 ± 92 pieces/ m^2).

Observed microplastic abundance has a large input from contamination, namely 1800 ± 960 pieces/kg dw (9540 ± 5088 pieces/m^2) (Fig. 3b). As a result, the actual microplastics concentration at each location is lower, reaching levels). The amount of contamination was variable during the extraction and characterization of the microplastics, indicated by the error bars (Fig. 3b). The highest amount of contamination can even eliminate the total amount of observed microplastic fibers at Stations 2, 3, 4 and 6.

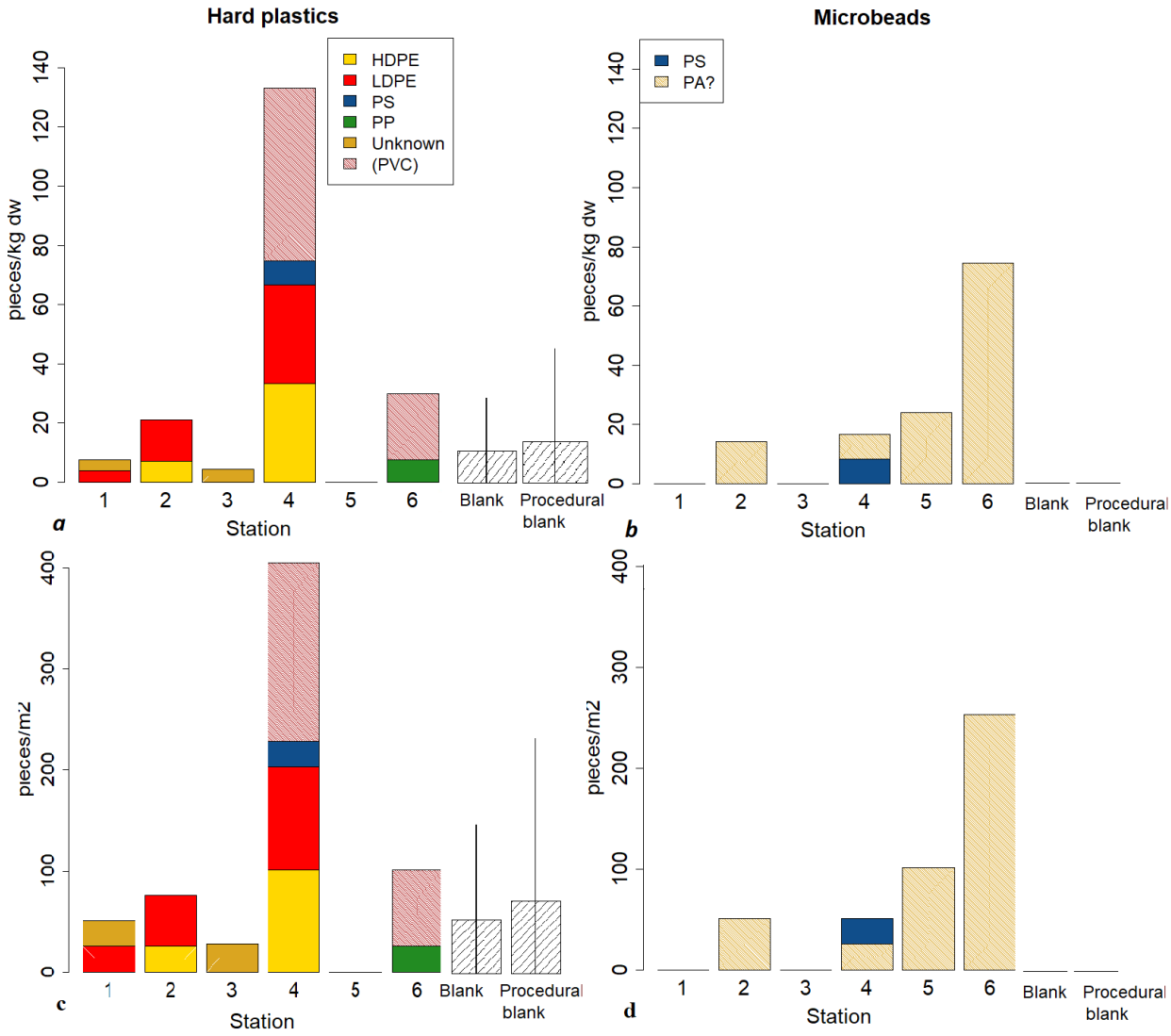

Figure 4. Distribution of (a) hard plastics and (b) microbeads along the depth transect. Polymers types present are: high-density polyethylene (HDPE), low-density polyethylene (LDPE), polypropylene (PP), polystyrene (PS), unknown, polyvinylchloride (PVC) and polyamide (PA). PVC is put between brackets as the spectra was of lower quality, thus not allowing for conclusive identification. A question mark is added to PA, as this identification is based on a visual comparison. Hard plastics of an unknown polymer type has been found in the blank, and HDPE in the procedural blank. Microbeads had no source of contamination.

The dominant source of contamination is from the SMI-unit (blank), with an average concentration of 1610 ± 917 pieces/kg dw (8549 ± 4860 pieces/m^2). This contamination consisted of both fibers and hard plastics, with a predominance of fibers (1600 ± 900 pieces/kg dw; 8480 ± 4770 pieces/m^2). The uncertainty in the degree of contamination is caused by the variance in the contamination of the SMI-unit. This contamination was controlled by performing the same procedure as for the extraction of microplastics, thus without sediment, 8 times for different SMI-units. A total of 30 extractions were performed to process all the samples. The blanks indicate the possible contamination of each extraction, but cannot be related to one single extraction. As a result, the variation of microplastic concentration observed in the blanks indicates a variable possible contamination of the samples.

The contamination in the fumehood and during the visual analysis was only by fibers, with concentrations of 120 ± 60 pieces/kg dw (636 ± 318 pieces/m^2) and between 20 to 170 pieces/kg dw (106 and 901 pieces/m^2) respectively.

3.2 Characterized microplastics

Subtracting contamination concentrations from the observed concentrations, microplastic fibers are present along the entire depth transect (Fig 3a) with the following concentrations from Station 1 to 6: 2698 ± 960, 749 ± 960, 353 ± 960, 875 ± 960, 1374 ± 960, 199 ± 960 pieces/kg dw (17995 ± 5088, 2578 ± 5088, 2124 ± 5088, 2663 ± 5088, 5824 ± 5088, 677 ± 5088 pieces/m^2). As a result of fibers being the dominant type of found microplastics, their abundance controls the distribution along the entire depth transect. Characterization of the fibers shows a dominance of transparent colored fibers at each station (46-62 %), followed by yellow (19-41 %) and black (10-11 %) (Fig. 5a). Station 5 deviates from this trend, as it shows a dominance in yellow fibers (42 %), followed by transparent (35 %) and black (9 %). The remaining fiber colors are white, blue, pink, red, green, grey and purple. Additionally, the color variety along the transect is different. The highest color variety is observed closest to shore (9 colors), lowest variety is at Station 6 (5 colors) as well (Fig. 6).

The observed color distribution is affected by the contamination as well. The dominant colors of the fumehood contamination are transparent (38%), black (30%) and blue (16%), while the dominant color of the contamination during the visual analysis is transparent (70 %) and pink (5 %) (Fig. 5c). As the contamination by both sources is relatively low, 100 pieces/kg dw and 140 pieces/kg dw respectively, their color distribution has a minor effect on the observed color distribution at each station.

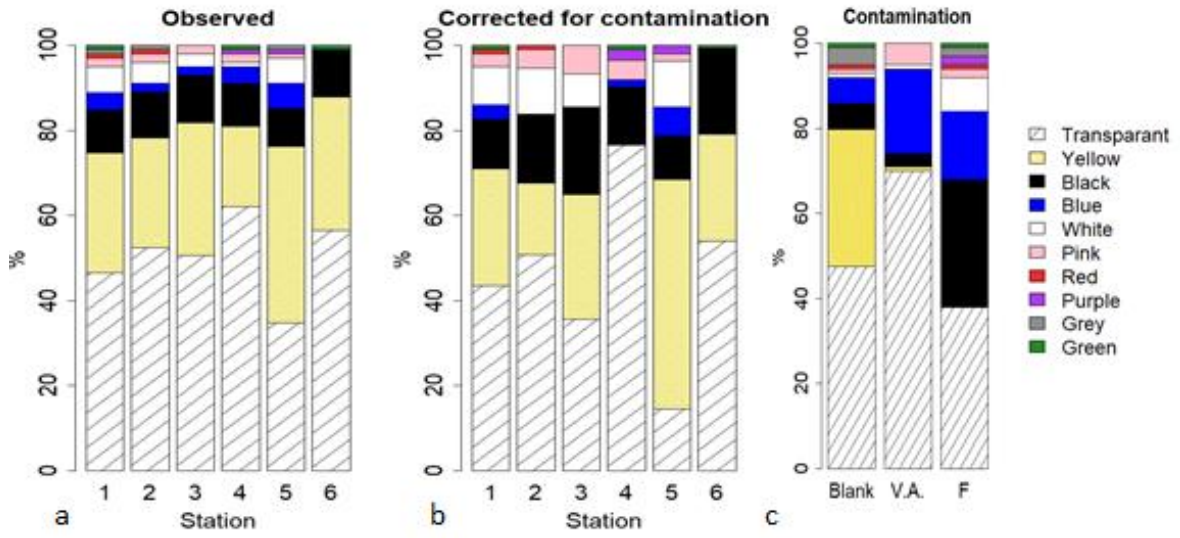

Figure 5. Color distribution of the fibers at each station a) observed, b) corrected for contamination, and c) the color for each source of contamination. V.A. stands for visual analysis and F for Fumehood. The correction for contamination has been done by subtracting the amount of fibers of each color counted at the blank, fumehood and visual analysis from the total amount counted of each fiber color.

In the blanks, transparent fibers were most dominant (47 %), followed by yellow (32 %), black (6 %) and blue (6 %) (Fig. 5c). Contamination by the blank was very significant (1610 ± 917 pieces/kg dw on average), therefore its color distribution has a larger effect on the observed color distribution (Fig. 5b). Overall, after the subtraction of the contamination, the transparent and yellow fibers became less dominant (36 and 51 %, 0 and 29 %, respectively), while the contribution of black and white slightly increased. All grey fibers were eliminated. The largest change is observed at Station 4, where no yellow fibers are present, and at Station 5 where yellow is the dominant color. At each station, the color variety decreased by 1 or 2 after contamination correction (Fig. 6)

Microplastics of type H have been found at each station, except at Station 5. With 4 pieces/kg dw (25 pieces/m^2), the concentration is lowest at Station 3, followed by Station 1 (8 pieces/kg dw; 51 pieces/m^2). With 133 pieces/kg dw (405 pieces/m^2), the concentration is highest at Station 4. Hard plastics are characterized as HDPE, LDPE, PP, PS, an unknown type of plastic and likely PVC (Fig. 4a). The spectra of PVC were of lower quality, thus not allowing for conclusive identification. Both buoyant (HDPE, LDPE and PP) and non-buoyant (PS and PVC) plastics were found. Spectra of identified microplastics can be found in Attachment 2.

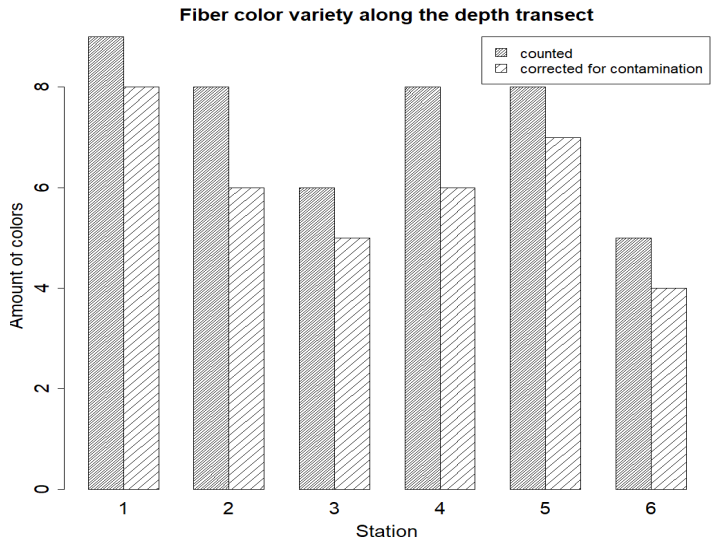

Figure 6. Color variety of the fibers at each station, both observed and corrected for contamination.

At the first two stations, only buoyant plastic polymers are present. At Station 4 the concentration of buoyant plastics (66 pieces/kg dw; 201 pieces/m^2) is highest. Here, non-buoyant plastics have been found as well, with a concentration of 67 pieces/kg dw (204 pieces/m^2). At Station 6, only non-buoyant plastics are present, with a concentration of 30 pieces/kg dw (101 pieces/m^2). The size of the hard plastics ranges from 180 to 643 µm.

Microbeads have been found at Stations 2, 4, 5 and 6, with increasing concentration moving offshore. From 14, 17, 24 to 74 pieces/kg dw (51, 51, 101, 253 pieces/m^2). With Raman analysis, one type of microbead has been identified as PS. Another type of microbead was burned with the Raman laser, while the spectra of another particle showed oscillation. Based on the visual comparison of a similar looking microbead found by Cole et al. (2015) the microbead is likely PA. The size of the microbeads ranges from 245 to 496 µm. A few of the potential microplastic particles were burned by the laser of the Raman (Fig. 7 m-p). The contamination ontrols of both the fumehood and the visual analysis show no contamination by hard plastics and microbeads.

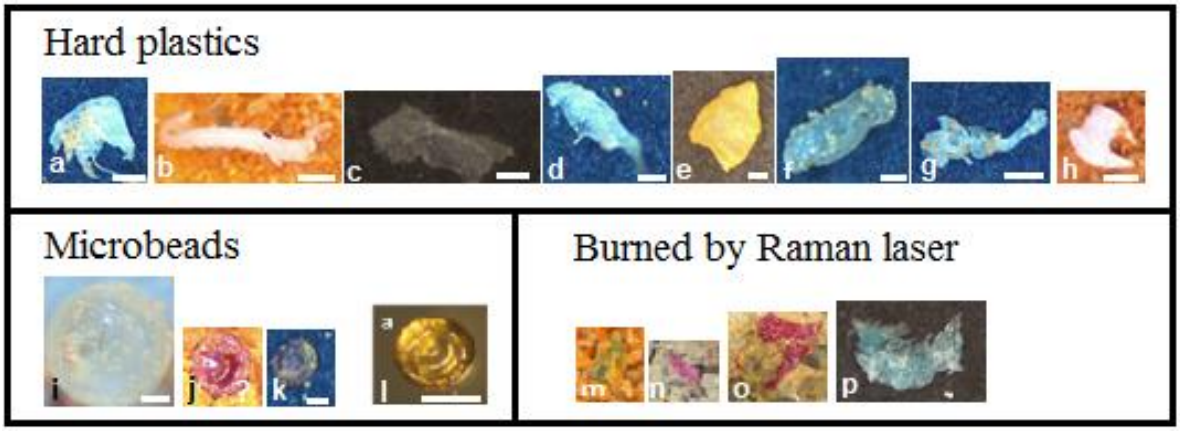

Figure 7. Pictures of found microplastics. The hard plastics are identified as: a,b) LDPE, c,d) HDPE, e) PP, f) PS, g) PVC, h) unknown. The microbeads are identified as: i) PS, j) unknown, k) PA (?), l) PA (Cole et al., 2015). Potential microplastics burned by the Raman laser: m, n, o, p. The white scale bar represents 100 µm.

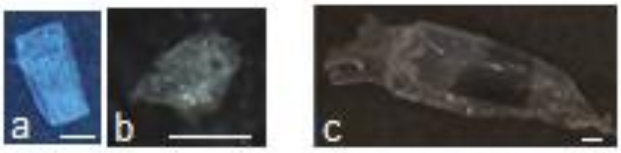

Figure 8. a,b) unknown hard plastics found at the blanks, c) HDPE from the procedural blank. The white scale bar represents 100 µm.

Two of the eight blanks had a concentration of 40 pieces/kg dw (212 pieces/m^2) of an unknown plastic type (Figs 4 and 8), given average contamination of 10 ± 17 pieces/kg dw (53 ± 92 pieces/m^2). Potentially, this can only affect the concentrations at Stations 1 and 3. From the six performed procedural blanks, one unit contained 80 pieces/kg dw (424 pieces/m^2) of HDPE, given an average of 13 ± 30 pieces/kg dw (71 ± 158 pieces/m^2). This could potentially eliminate the found observed HDPE at Stations 1 and 4. The fiber concentration at the procedural blank was 440±120 pieces/kg dw (2332 ± 636 pieces/m^2).

3.3 Reviewing the method

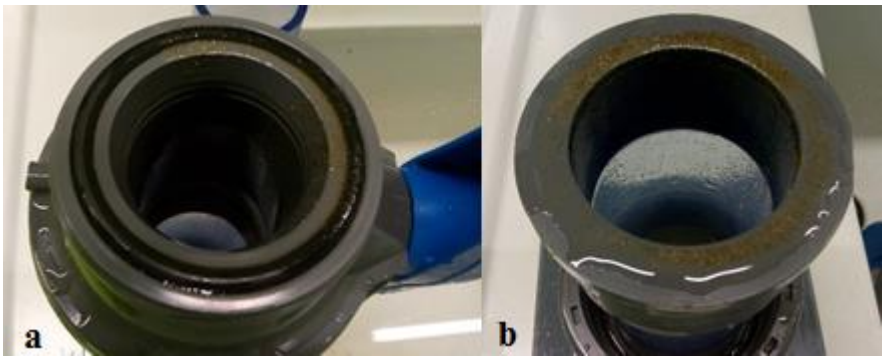

Figure 9. Sediment trapped between the compartments of the SMI-unit, a) at ball valve, b) at lower compartment. This indicates a potential loss of microplastics.

During the extraction and characterization of microplastic particles, there was a potential loss of particles. First of all, disassembling of the SMI-unit after the density separation showed that sediment was trapped in between the three compartments (Fig. 9). This loss has not been reported by Coppock et al. (2017), but might affect the reported recovery rate of 95%. Besides the microplastics, sediments with a grain size between 30-100 µm (estimated) and calcareous material were extracted too. The latter was removed by decalcification. But in general, the presence of non-plastics decreased the quality of the visual analysis.

Decalcification with 1M HCl did not result in a change in the total weight (thee decimals accuracy) of the tested microplastic particles. Moreover, visual comparison by light microscopy of the surface of the particles before and after the exposure to 1M HCl showed that degradation did not occur. Exposing the samples for a maximum duration of 15 minutes was sufficient to remove all calcareous material. As a result, the visual analysis improved significantly due to the decalcification. This method has thus proved to be effective in removing calcareous material without degrading microplastics. Therefore, this methodology is reliable for decalcifying samples and improving the visual analysis. Fischer et al. (MICRO, 2018) showed that even 10% HCl (3.24 M) can be used for decalcification in microplastic research, without degrading plastics.

Before the decalcification of the sample of Station 5, no microplastics were observed. However, as a result of the decalcification 24 pieces/kg dw (509 pieces/m^2) microbeads, a red and blue hard plastics (Figs. 7o, p) were observed. No fumehood control has been performed during the decalcification, but it is unlikely the observed microplastic particles are a result of contamination as no microbeads or hard plastics have been observed at any fumehood control.

Löder and Gerdt. (2015) reported that visual analysis with a microscope is most reliable for particles with a size larger than 500 µm. For smaller particles, the error rate varies between 20 to 70% due to misidentification of the particles and loss of particles when transferring from the sample to the cardboard. This rate increases with decreasing particle size. In this study, 69 % of the observed particles have a size smaller than 500 µm. This explains the loss of 19 ± 8 % of the particles during the transfer from the sample to the filter or cardboard (Table 7). As a consequence of this loss, the concentration of observed hard plastics and microbeads could be potentially up to 30% higher (Table 7). Due to this loss of particles and to reduce the time for the visual analysis, not all potential microplastics were transferred to the cardboard. Instead of this, particles with a similar appearance were noted. This could result in potential misidentification as polymers can have a similar appearance.

The low concentrations of hard plastics and the absence of microbeads at Station 1 are likely biased by the loss of a fraction of these particles during the visual analysis. 29% of the sample was flipped on top of the table and 30% was lost when transferring the particles to the cardboard. Potential microplastics are lost during the Raman analysis as well. Particles with the colors red, pink, green and blue were very sensitive to the laser intensity. A low intensity did not result in a spectrum, while a higher laser intensity fully burned the particle.

Contamination in the fumehood and during the visual analysis do not show a large variation (Fig. 3), and therefore can be estimated well. Based on the blanks, there is no contamination of hard plastics and microbeads of a known plastic type. The procedural blanks did, however, show the presence of hard plastics identified as HDPE. This could be a source of contamination coming from the degradation of the ball valve. PVC has not been found in the blanks. Therefore, it is very unlikely that the observed PVC in the samples is coming from contamination. Observed hard plastics can have a source of contamination, but this is accounted for by the blanks. Therefore, the used methodology is reliable to obtain the data for hard plastics in sediment.

Table 7. Loss of particles during the visual analysis of the particles, when transferring the particles from the sample to the filter or cardboard. This percentage has been derived from the total number of particles transferred and the amount lost during this transfer.

	St. 1	**St. 2**	**St. 3**	**St. 4**	**St. 5**	**St. 6**
Visual analysis (%)	30	13	19	5	26	20

As microbeads do not have a source of contamination, the used method is fully reliable. The used method makes it impossible to be certain whether or not the found microplastics come from contamination. The observed findings can only be compared to what is found in the blanks. To add certainty to the observations, Raman spectra of each source of contamination (Table 5) should be made. The spectra of microplastics found in the samples should be compared to those spectra. Spectra of products made of a similar polymer type can deviate from each other as a result of plastic additives. This will make the spectrum of each contaminant unique.

The large variety in the amount of contamination by fibers has a large effect on the results. At each station, a minimum to average amount of contamination, fibers are the dominant type of microplastics. While with maximum contamination, fibers would be absent at Stations 2, 3, 4 and 6. Therefore, the concentration of fibers along the depth transect is highly uncertain, and the used method is not suitable to give a reliable estimate of the fiber concentration. The high uncertainty shows that it is very important to rinse the SMI unit thoroughly after each extraction and check the filter for potential contaminants after the addition of $ZnCl_2$ and filtering. Making the SMI-units free of contaminants before usage was not that easy. The process of adding $ZnCl_2$, leaving for 10 minutes, filtering and inspecting the filters were performed more than 8 times for each SMI-unit. Still, white and transparent particles were visible on the filters. This appeared to be glue. The high concentration of fibers at the blank could indicate that the SMI-units were not clean enough. Visual inspection by eye might be not sufficient enough as a check if the SMI-units were contaminant free. Therefore, it is advised to check the filters under the light microscope for contaminants. In addition, the amount of contamination from the SMI-units can be halved by adding a double amount of sediment (50 g) to the SMI-unit for each extraction. According to the protocol of Coppock et al. (2017), the method is still reliable with the addition of 50 g of sediment (dw) to the SMI-unit. Contamination of the fibers should be reduced as much as possible, although it can never be fully ruled out due to its presence in the air and Milli-Q water.

Methods to perform automatic analysis to identify and characterize microplastics are in development (Primpke et al., 2017; Renner et al., 2017). Such a method would be more reliable, as there is no loss of potential microplastic particles, no human bias and reduced risk of contamination.

Ideally, the time interval over which the microplastics have been deposited was calculated for each site. Unfortunately, this is not possible because the sedimentation rate was not available yet.

4. Discussion

As discussed before, microplastics are extracted and identified according a variety of methods affecting the obtained microplastic concentration. To be able to compare the microplastic concentrations reported by different studies properly, an overview of the used methods, measured concentrations and identified microplastics given (Tables 8 to 13). In addition, microplastic concentrations are given in pieces/kg dw and pieces/m^2, if possible. Reported microplastic concentrations in pieces/m^2 are converted to pieces/kg dw and vice versa (according to Equation 2).

4.1 Microplastic distribution along the depth transect

Microplastics have been found along the entire depth transect with concentrations varying between 303 ± 960 and 2705 ± 960 pieces/kg dw (1031 ± 5088 and 18046 ± 5088 pieces/m^2). Highest concentrations were observed at Station 1, even though 29% of that sample was lost. Similar concentrations have been observed in marine sediments at the Mediterranean Sea (Alomar et al., 2016; Abidli et al., 2018) and the Lagoon of Venice (Vianello et al., 2013), between 100 and 897 pieces/kg dw (757-6792 pieces/m^2) and 672 to 2175 pieces/kg dw (3562-11527 pieces/m^2) respectively. (Tables 8 and 9) Concentrations over 2000 pieces/kg dw have not been much reported. With a depth of 2100 mbss, Station 6 is located in the deep sea. Minimum data about microplastic accumulation at this depth is available. Microplastic concentrations at deep-sea sediments have been reported at the Porcupine Abyssal Plain, Atlantic sector Southern Ocean and Nile deep-sea fan in concentrations between 7.5 and 15.1 pieces/kg dw[1] (200 and 400 pieces/m^2), and at the Arctic in concentrations between 42 and 6595 pieces/kg dw (200 and 34954 pieces/m^2) (Van Cauwenberghe et al., 2011; Bergman et al., 2017; Tables 8 and 9). In these studies, microplastic fibers were not included. The microplastic concentration at Station 6, excluding fibers, is 104 pieces/kg dw (354 pieces/m^2) and is thus higher than observed at several locations worldwide but is in the lower range of observed concentrations at the Arctic deep-sea.

Measured microplastic concentration highly depends on the minimum size that can be extracted with the method. Bergman et al. (2017) reported that 80% of the found microplastics were smaller than 25 µm. This implicates that microplastic concentrations found in this study (>30 µm) are likely underestimated.

[1] Converted from the reported concentration in pieces/25 cm^3 by assuming a sediment density of 2.65 g/cm^3.

Table 8. Studies performed to microplastics performed across the world, their location, the sample type, surface area and depth of the taken samples, and the used methods. FTIR = Fourier Transform Infrared spectroscopy, ATR = Attenuated total reflectance, MPSS = Microplastic sediment separator.

Study	Location	Sample type	Sample area and depth	Method
This study	Mississippi River delta. A transect from the river mouth to offshore	Marine sediments	79 cm^2, 5 cm depth	Density separation $ZnCl_2$ (1.5 g/cm^2). Visual analysis, Raman-spectroscopy
Van Cauwen-berghe et al., 2011	Nile deep-sea fan	Marine sediments	25 cm^2, 1 cm depth	Sieving, density separation (NaI, 1.6 g/cm^3), visual analysis, Raman
	Porcupine Abyssal Plain	Marine sediments	25 cm^2, 1 cm depth	Sieving, density separation (NaI, 1.6 g/cm^3), visual analysis, Raman
	Atlantic sector Southern Ocean	Marine sediments	25 cm^2, 1 cm depth	Sieving, density separation (NaI, 1.6 g/cm^3), visual analysis, Raman
Claessens et al., 2011	Belgium coast	Marine sediments	0.1 m^2, 70 kg	Density separation (concentrated saline solution), visual analysis, FTIR
Alomar et al., 2016	Mallorca	Marine sediment	3.5 cm diameter, 0-3.5 cm depth	Sieving, density separation (-), visual analysis
Abidli et al., 2018	Tunesian coast	sediments	0.25x0.25 m, 2-3 cm depth.	density separation (NaCl, 140 g/L), visual analysis, FTIR-ATR
Vianello et al., 2013	Lagoon of Venice, Italy	sediment 1 mbss	5 cm depth	density separation (120 g/L NaCl), ATR-uFT-IR
Blumen-röder et al., 2017	Orkney, N Scotland	intertidal sediments	top 3 cm, 5ml jar	density separation NaCl (384 g/L), visual analysis, FT-IR
Bergmann et al., 2017	Arctic	Sediments (deep-sea)	100 mm diameter, 5cm depth	MPSS, density separation $ZnCl_2$ (1.7-1.8 g/cm^3), visual analysis, ATR-FTIR
Nor and Obbard, 2014	Singapore coastal mangrove	Sediments	2.25 m^2, 3-4 cm depth	Density separation NaCl (1.18 g/cm^3), Visual analysis, ATR-FTIR

*Table 9. Studies performed to microplastics performed worldwide, the obtained concentrations, the size and type of microplastics (H= hard plastics, B = microplastics, **Fb**= fibers, P= pre-produced pellets) and the polymer types (HDPE = high-density polyethylene, LDPE = low-density polyethylene, PE = polyethylene, PP = polypropylene, PS = polystyrene, PA = polyamide, PET= polyethylene terephthalate, PEst = polyester, PVOH = polyvinyl alcohol, PTFE = polytetrafluoroethylene). Concentrations are given in both pieces/kg dw and pieces/m^2. Values in black are as reported in the paper, values in red are the converted values according to equation 2. Conversion from pieces/kg dw to pieces/m^2 has been done for a depth of 1 cm.*

Study	**Concentration (unit)**	**Size (µm)**	**Types of plastics**	**Polymer types**
This study	303 ± 960 – 2705 ± 960 pieces/kg dw 1031 ± 5088 – 18046 ± 5088 pieces/m^2	180 – 643 (>30µm)	**Fb**, H, B	HDPE, LDPE, PP, PS, PVC, PA, unknown
Van Cauwen-berghe et al., 2011	7.5 pieces/kg dw 200 pieces/m^2	75	H	Not specified
	7.5 pieces/kg dw 200 pieces/m^2	75	H	Not specified
	7.5 pieces/kg dw 200 pieces/m^2	75	H	Not specified
Claessens et al., 2011	67-390 pieces/kg dw 1776-1-335 pieces/m^2	> 38	**Fb**, H, B	Nylon, PVOH, PP, PS, PE, PP
Alomar et al., 2016	100-897 pieces/kg dw 757-6792 pieces/m^2	> 63	**Fb,** H	Not specified
Abidli et al., 2018	141-461 pieces/ kg dw 1495 – 4889 pieces/m^2	> 100	**Fb**, H, P	PE, PP, PS
Vianello et al., 2013	672-2175 pieces/kg dw 3562-11528 pieces/m^2	15- 2413	H, **Fb**, P	PE, PP, PEst, PS, PAN, alkyd, PVC, PVOH, PA
Blumen-röder et al., 2017	730-2300 pieces/kg dw 6448-20317 pieces/m^2	> 0.7 µm	**Fb**, H	PTFE, PE, PVC, PA
Bergmann et al., 2017	42 and 6595 pieces/kg dw 200 and 34954 pieces/m^2	> 1 µm	H, B	PTFE, PP, PE, PA, PP, nitrile rubber
Nor and Obbard, 2014	12.0 ± 8.0 – 62.7 ± 27.2 pieces/kg dw 90.6 ± 60.6 - 474 ± 205.9 pieces/m^2	> 1.6 µm	**Fb,** H, B	PP, PVC, nylon, PE

Our findings are in agreement with the general observation that fibers are the most dominant type of microplastic found in marine sediments worldwide, with concentration varying between 12 and 325 pieces/kg dw (91 and 2461 pieces/m^2) (Claessens et al., 2011; Nor and Obbard, 2014; Alomar et al., 2016; Abidli et al., 2018; Tables 8 and 9). Observed fiber concentrations are in the same order of magnitude and 1 order of magnitude higher. In this study, fibers control the observed trend in microplastic distribution along the depth transect. Due to the high variability in the fiber contamination, the reported concentrations of both fibers and total microplastics are highly uncertain. According to the range, the contamination at one station can potentially be up to a factor of 3 higher compared to another. As a result, the observed trend is also uncertain. With the method used, the reported concentrations can only be discussed in the order of magnitude.

Hard plastics are present along the entire depth transect, except at Station 5. Concentrations range from 4 to 133 pieces/kg dw (25 and 405 pieces/m^2). The irregular shape of the hard plastics suggests that they are all of secondary origin (Fig. 7). Hard plastics found in beach sediments of the estuary at Mobile Bay (Northern Gulf of Mexico) were also only secondary microplastics (Wessel et al., 2016). This observation is likely related to the residence time of water at the Mississippi and Gulf of Mexico. The residence time for water of the Mississippi river varies is less than 1 for 66% of the water and 10 years for the remaining 33%, with its origin from long-term reservoirs (Michel, 1992). The residence time at the Gulf of Mexico varies between 3 months and 250 years (Rivas et al., 2005). An increased residence time gives more time for the accumulated plastics to degrade and fragment into smaller particles. Therefore, it is expected that most secondary plastics are formed at the long-term reservoirs of the Mississippi River and at the waters of the Gulf of Mexico.

Microbeads have been found at Stations 2, 4, 5 and 6, with concentrations ranging from 14 to 74 pieces/kg dw (51 and 253 pieces/m^2). Sources of primary microbeads are cosmetics such as scrubs, facial cleaner and toothpaste, and air-blasting technology (Zitko and Hanlon, 1991; Gregory et al., 1996). With a microplastic settling velocity between 5 – 127 mm/s, microplastics could reach a depth of 16 mbss within 2 to 53 minutes (Khatmullina et al., 2017), and for a depth of 2100 mbss, this will take 4.6 to 117 hours. Furthermore, an experiment of Khatmullina et al. (2017) reported that spheres (representing B) have a higher settling velocity compared to isometric cylinders (represents H) and fibers.

With this knowledge, microbeads are expected to be present at the stations close to the shore, brought in by riverine water of the Mississippi and Atchafalaya. The turbulence of the water close to shore might have kept the microplastics in the surface layer (Nickols, 2009), and could explain the absence of microplastics at Stations 1 and 3.

The size of the hard plastics and microbeads are smaller than the 2.2 mm, and so fall in the size range of 'missing' floating plastics. Microplastics smaller than this 2.2 mm have been suggested to experience size-selective sinking from the surface water to deeper waters or the seabed (Cózar et al., 2014). The size of microplastics found at the marine sediments of the MRD supports that the seabed might be a sink for this missing plastics.

4.2 Characterized microplastics

The color distribution of fibers is different per study site. In this study, transparent, yellow and black fibers dominated. Other studies report also the dominance of transparent, black, blue and white fibers (Reisser et al., 2013; Alomar et al., 2016; Blumenröder et al., 2017; Abidli et al., 2018). Characterization of fibers by color is faster and cheaper than identification with Raman or FT-IR. But visual analysis could result in false positive and false negative results (Lenz et al., 2015). Lenz et al. (2015) and Silva et al. (2018) showed that 65% to 75% of visually identified plastics were also identified as plastic with Raman or FTIR. Therefore, the number of plastic fibers present at the Gulf of Mexico is likely 25% to 35% lower.

Hard plastics of both buoyant (HDPE, LDPE, PP) and non-buoyant polymer (PS, PVC) types have been found along the depth transect. The polymer types observed at the seabed in this study corresponds to general findings of the polymer types (PE, PP, PS) of microplastics in sediments (Vianello et al., 2013; Blumenröder et al., 2017; Abidli et al., 2018; Tables 8 and 9). PE, PP and PS have been found in skin cleansers (Zitko and Handlon, 1991).

A concentration of 40 pieces/kg dw (1060 pieces/m^2) of an unknown plastic type (of type H) has been found in 2 out of the 8 blanks. This concentration is higher than the observed concentration of unknown plastic in our sample. Therefore, these particles are likely introduced by contamination. Testing the degradation of the SMI-units has been done by the so-called procedural blanks. In one of the six procedural blanks, 80 pieces/kg dw (2120 pieces/m^2) of HDPE has been found. Therefore, HDPE present in our samples might be a source of contamination as it can be a product of the degradation of the SMI unit. Although not observed as a degradation product of the SMI unit (blanks and procedural blanks), PVC is a potential source of contamination too (Table 5).

As a result of these sources of contamination, concentrations at Stations 1, 2, 4 and 6 are likely lower. And microplastics could even be absent at Station 3. Making Raman spectra of all sources of contamination made from of HDPE and PVC and comparing it to the spectra of found microplastics in the samples will give a conclusive answer if the found microplastics are input from contamination or not.

For microbeads, only polymer types with a higher density than seawater (PS, PA?) have been found. Claessens et al. (2011) reported the same.

4.3 Sources of microplastics and transport mechanisms

Rivers contribute greatly to ocean plastics worldwide (Jambeck et al, 2015; Lebreton et al., 2017). As the Mississippi-Atchafalaya basin drains 40% of the continental US, it is very likely an important source of plastics at Gulf of Mexico. 71 million people reside in this basin, the area is highly industrialized, used for agricultural purposes and about 7000 wastewater treatment plants are located in this basin. The high microplastic concentration, due to a high concentration of fibers at Station 1 can be explained by its location close to the shore. The effluent of washing machines is an important source of fibers in rivers, and likely contributed to the high amount of fibers found close to shore (Browne et al., 2011; Claessens et al, 2011; Vermair et al., 2017). A single garnet per wash can produce 1900 fibers (Browne et al., 2011). Fibers have also an origin at sea. Where fibers are produced from the fragmentation of ropes, lines and fishing nets and coming from the effluent of washing machines on boats (Andrady et al., 2011).

The microplastic concentration does not show a direct correlation with the depth (R^2 = 0.3524618, Fig. 10). The correlation between the microplastic concentration and the distance from the coast is slightly better (R^2 = 0.4823874, Fig. 11). One factor that contribute to the observed distribution of microplastics along the transect, are the prevailing surface currents, driven by the global wind system (Ocean currents, 2018), at the northern Gulf of Mexico (Fig. 12). Surface currents are shown to play an important role in the distribution of (micro)plastics (Lebreton et al., 2012; Blumenröder et al., 2017). A surface current flows from the Mississippi River mouth along the coast in a westward direction (Fig. 12). Station 1 is located within this current, and therefore it can be concluded that the Mississippi River is the main source of microplastic, also considering the high concentration of fibers. Based on the surface currents, Station 1 has likely input from the Atchafalaya river as well.

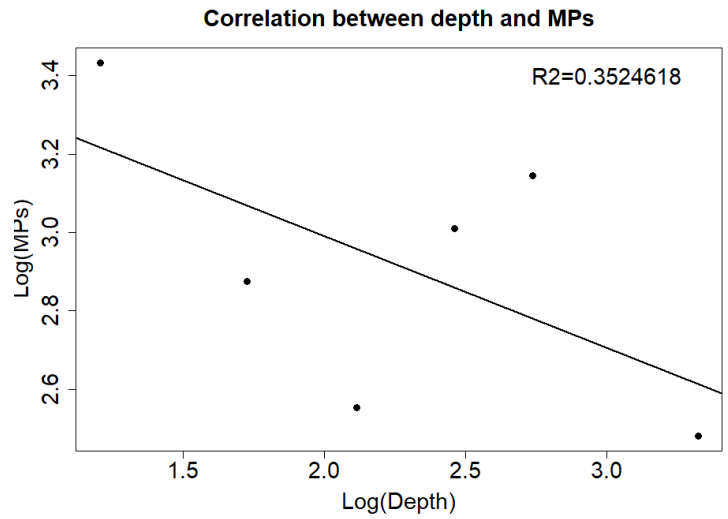

Figure 10. Microplastic concentration (MPs) as a function of the sample depth, plotted as logarithmic values. R^2 is the correlation coefficient between the microplastic concentration and sample depth.

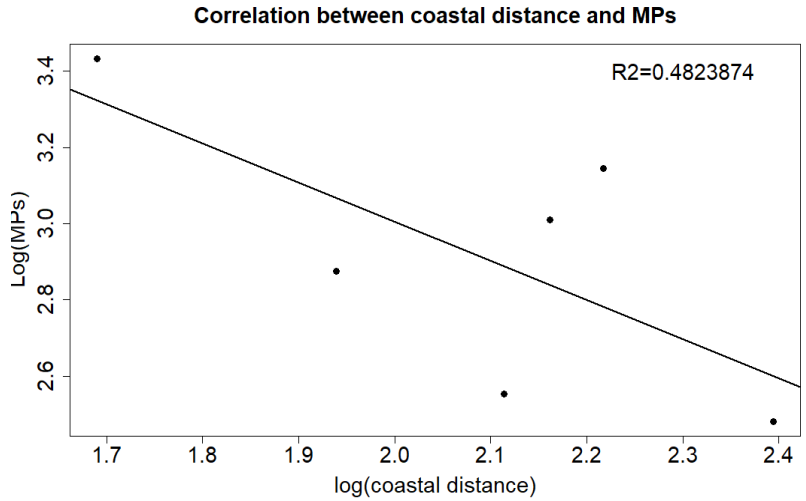

Figure 11. Microplastic concentration (MPs) as a function of the distance from the coast, plotted as logarithmic values. Estimated distances for station 1 to station 6 are: 48, 87, 130, 145, 165 and 248 km. R^2 is the correlation coefficient between the microplastic concentration and distance from the coast.

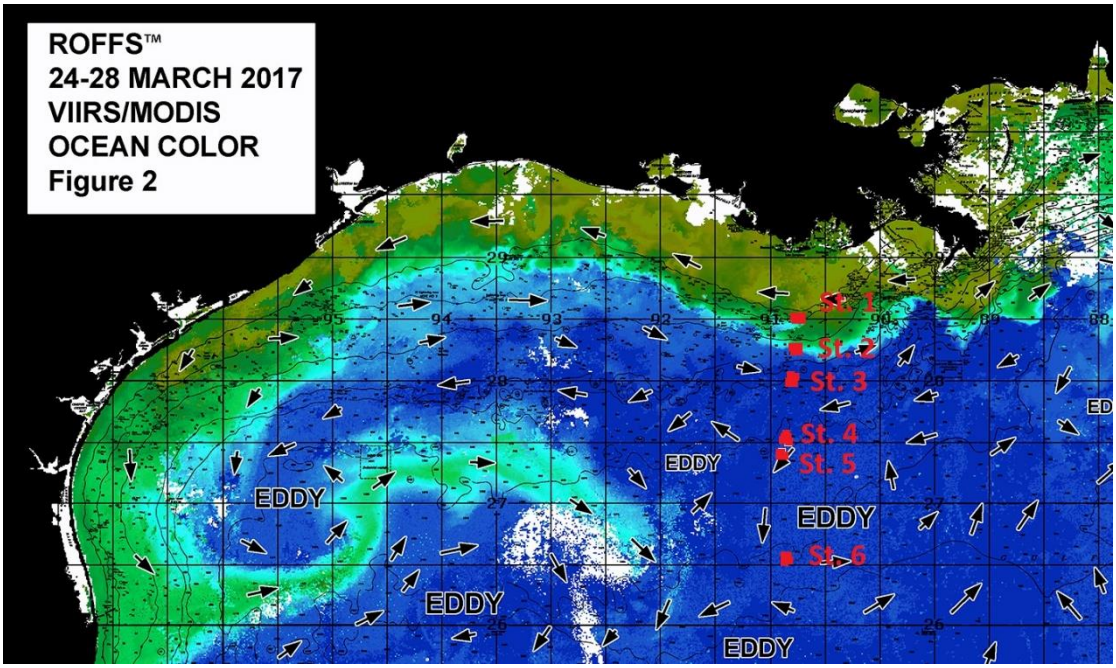

Figure 12. Surface currents at the northern Gulf of Mexico. The locations of stations 1 to 6 are indicated by red points.

Parallel to the westward-coastal current, a surface current flows in opposite direction back to the Mississippi river mouth. Here, Station 3 is located. At the West of this opposite surface current, there is no major riverine input. Only the city of Houston could potentially act as a source. However, the along-shore current could transport this to the South. Likely, the countercurrent has its origin partly at the Mississippi mouth. Based on these observations, the countercurrent has likely a lower concentration of microplastics compared to the current along the shore, as it is expected that fibers are removed from the surface water along their way. This will explain why concentrations of fibers at Station 3 are much lower. Nonetheless, there is no data to prove this hypothesis. Station 2 is located between the two surface currents, and so likely has input of both, explaining the observed intermediate concentration. To prove the hypothesis that microplastic concentrations at the 'opposite current' is low, surface water samples at this current should be taken. At least at a location most West and a location in between that point and the Mississippi river. However, sampling along this entire current should provide more detail about the microplastic concentration in the surface waters of this current. In addition to the surface currents, underwater currents, driven by differences in water density, played a role in the distribution of microplastics as well, as those currents have their own flow pattern (Ocean currents, 2018).

Stations 4, 5 and 6 are located at the outer margins of a cyclonic eddy (Fig. 12, Oey, 2007). Eddies can accumulate particles from the surrounding surface waters, and as a result microplastic concentrations could increase over time. Cyclonic eddies have the tendency to accumulate particles at the outer margins of the circulation (Walker et al., 2011). The position of Stations 4, 5 and 6 at the outer margins of this cyclonic eddy might explain the higher concentration of microbeads. A model study of microplastic distribution in the Gulf of Mexico by Yu et al. (2018) came to a similar conclusion. Based on the varying flow directions of the currents around the eddy (Fig. 12), the microplastics observed at the locations of this eddy likely have different sources. Based on this argumentation, the lower concentration of microplastics at Station 6 and the absence of hard plastics at Station 5 cannot be explained. The differences in microplastic composition at locations along the edges of the eddy might be explained by the varying flow of surface currents around the eddy, bringing plastics from different areas. Striking is that the microplastic composition at Stations 4 and 6 contains relatively high amounts of hard plastics and microbeads compared to the other stations.

In addition to the currents, the geography is an important factor controlling the microplastic distribution. First of all, highly populated area like the cities New Orleans, Houston, Galveston and Mobile, acting as source for plastic pollution. Second, Wessel et al. (2016) reported higher concentrations at estuarine beach sediments with a larger marine influence, by currents. They suggest that this is related to the residence time of plastics in the Gulf of Mexico, which is between the 3 months and 250 years (Rivas et al., 2005). Increased residence time increases the time for plastics to degrade and fragment into smaller particles. They conclude that exposure to currents of the Gulf of Mexico likely indicates the presence of MP along the shoreline. From this can be concluded that microplastics formed as a result of the breakdown of larger plastics at the surface waters of the Gulf of Mexico too, and are therefore is likely an important source as well.

The more dominant polymer types of hard plastics have a lower density than sea-water. For that reason, a process must be involved to increase the density of the microplastic particles in order to eventually be able to sink to the seabed. PS (both H and B) and PA have a higher density than seawater and could be transported downward by directly sinking. Biofouling has been reported to be an important pathway for vertical transport (Wright et al., 2013; Cózar et al., 2014; Kooi et al., 2017).

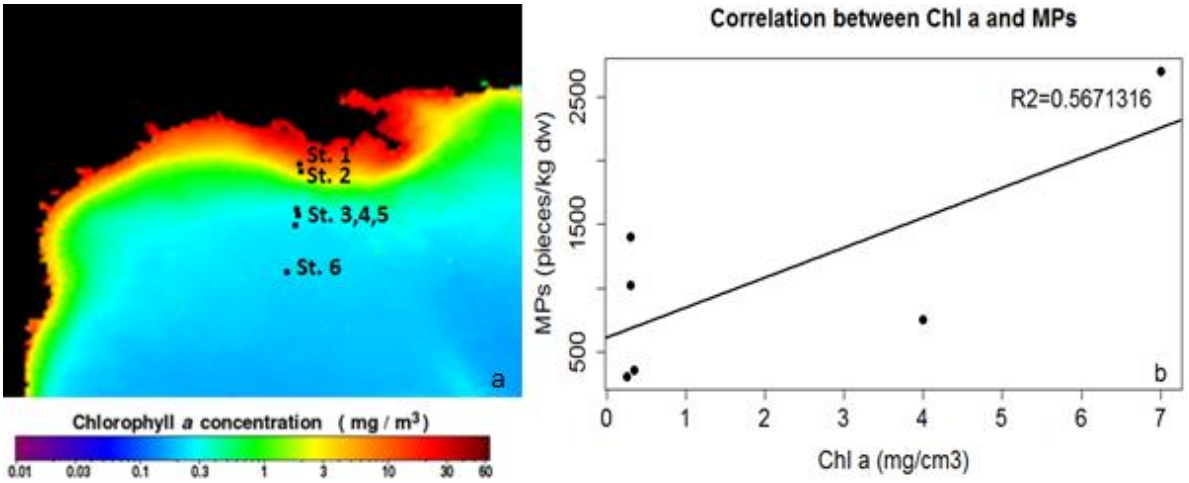

Figure 13.a) Chl a concentration as an indication for primary productivity at the Northern Gulf of Mexico. SeaWiFS- entire mission composite 1997-2010 (adapted from https://svs.gsfc.nasa.gov/30801 ,), b) Microplastic concentration as a function of Chl a

The map with the average chlorophyll *a* concentration over 13 years (Fig. 13 a), an indicator for primary productivity, shows a relative high productivity (6 and 15 mg/m^3) at Stations 1 and 2, and very minor productivity (<0.3 mg/m^3) at the 4 stations further offshore. The microplastic concentrations in this study show a minor linear correlation between Chl *a* concentration at this region (R^2= 0.5671316, Fig. 13 b). Based on this correlation and the high Chl a concentration at Stations 1 and 2, biofouling could potentially occur at these stations and likely contributed to the transport to the seabed. Lower Chl *a* concentrations at Stations 3 to 5 compared to Stations 1 and 2, meaning less productive water, indicate a lower potential for biofouling. The potential is even lower at Station 6, located at the deep-sea. Another way of vertical transport is by the formation of marine snow (Alldredge and Silver, 1988; Porter et al., 2018). But, this remains speculative, as there is no data available for this study.

4.4 Sinks of microplastics in the Gulf of Mexico

Data on microplastic abundance on the seabed, in beach sediments, in surface waters and in the ocean water column at the Gulf of Mexico is scarce. Here, we have reported for the first time the microplastic concentration at the seabed of the Gulf of Mexico, both in pieces/kg dw and pieces/m^2. Reported concentrations from beach sediments vary from 0.11 to 443 pieces/kg dw (13.2 – 7826 pieces/m^2) (Wessel et al., 2018; Yu et al., 2018; Tables 10 and 11), fibers included. The concentrations are highly influenced by the location.

Table 10. Studies performed to microplastics performed at the Gulf of Mexico, their location, the type of samples taken (both sediments and water), surface area and depth of the samples, and the used methods. FTIR = Fourier Transform Infrared spectroscopy, ATR = Attenuated total reflectance.

Study	Location	Sample type	Sample area and depth	Method
		Sediments		
This study	Mississippi River delta. A transect from the river mouth to offshore	Marine sediments	79 cm^2, 5 cm depth	Density separation ZnCl2 (1.5 g/cm^2). Visual analysis, Raman-spectroscopy
Wessel et al., 2016	Mobile Bay, Northern GOM	Beach, estuary *freshwater* influenced	0.25x0.25m, 3 to 6 cm depth	Density separation, 35 psu water. Visual analysis, ATR-FTIR
		Beach, estuary *marine* influenced		
Yu et al., 2018	Northern GOM. Close to Alabama River, N. of Rio Grande, S. Florida	Beach	25 cm diameter, 1,5 cm depth	Density separation, NaCl (1.27 g/cm^3), Visual analysis, FTIR
		Water		
Lebreton et al., (2012)	GOM	Surface	-	model
Eriksen et al., (2014)	GOM	Surface	-	model
Van Sebille et al. (2015)	GOM	Surface	-	model
Mauro et al., (2017)	Front Mississippi Delta, GOM	Surface and water column	0-15m depth, 0-0.4m depth. Both 60cm diameter; 5L	Bongo and neuston (335 µm mesh size), niskin bottle (0.7 µm), FTIR
Lecke-Mitchell and Mullin (1997)	GOM	Surface	-	Aerial surveys cetaceans

*Table 11. Studies performed to microplastics performed at the Gulf of Mexico (both sediments and water), the found concentrations, the size and type of microplastics (H= hard plastics, B = microplastics, **Fb**= fibers) and the polymer type (HDPE = high-density polyethylene, LDPE = low-density polyethylene, PE = polyethylene, PP = polypropylene, PS = polystyrene, PA = polyamide, PET= polyethylene terephthalate). Concentrations are given in both pieces/kg dw and pieces/m^2. Values in black are as reported in the paper, values in red are the converted values according equation 2. Conversion from pieces/kg dw to pieces/m^2 has been done for a depth of 1 cm.*

Study	**Concentration (unit)**	**Size (µm)**	**Types of plastics**	**Polymer types**
Sediments				
This study	303 ± 960 – 2705 ± 960 pieces/kg dw 1031 ± 5088 – 18046 ± 5088 pieces/m^2	180 - 643	**Fb**, H, B	HDPE, LDPE, PP, PS, PVC, PA, unknown
Wessel et al., 2016	0.11 ± 0.02 pieces/kg dw 13.2 ± 2.96 pieces/m^2	200-2800	H, all secondary. **Fb**, B	PE, PP, PS, PA, polyester
	0.42 ± 0.09 pieces/kg dw 50.6 ± 9.96 pieces/m^2	2000-3500	H, all secondary. **Fb**, B	PE, PP, PS, PA, polyester
Yu et al., 2018	253-443, 196-253, 43-123 pieces/kg dw 4470-7826, 3463-4470, 760-2173 pieces/m^2	>1 µm	**Fb**, H, B	PET
Water				
Lebreton et al., (2012)	0.01-0.1 pieces/m^2	Not specified	Floating debris	Not specified
Eriksen et al., (2014)	0.2 pieces/m^2	33 -4750	H, **(Fb?)**	Not specified
Van Sebille et al. (2015)	0.1-1.0 pieces/m^2	>150	Not specified	Not specified
Mauro et al., (2017)	4.8 - 8.2, 5.0-18.4 pieces/m^3; 0.048- 0.082, 0.050- 0.184 pieces/m^2 [2] (Bongo, neuston, respectively)	Cross-section-al area 10E-3 – 10E-1 (mm^2)	**Fb.** H, B.	Not specified
Lecke-Mitchell and Mullin (1997)	1E-6 (pieces/m^2)	Micro and macro	Marine litter	Not specified

[2] Microplastic concentration per surface area for a depth of 1 cm.

Highest concentrations in beach sediments are found close to the Alabama river with 253 to 443 pieces/kg dw (4470-7826 pieces/m^2), followed by North-West of the Gulf of Mexico between 196- 253 pieces/kg dw (3463-4470 pieces/m^2) and South Florida between 43-123 pieces/kg dw (760-2173 pieces/m^2). Concentrations are much lower at the Mobile bay estuary, with 0.11 to 0.42 pieces/kg dw (13.2-50.6 pieces/m^2). Highest concentrations at the Mobile bay is observed at sites with a strong marine influence. Concentrations at Stations 1, 2, 4 and 5 are a factor 2 to 60 times higher than reported for beach sediments in the Gulf of Mexico.

Model studies estimate a concentration between 0.01 and 1 pieces/m^2 at the surface waters of the Gulf of Mexico (Lebreton et al., 2012; Eriksen et al., 2014; Sebille et al., 2015; Tables 10 and 11). Microplastic concentration in the upper 40 cm of the surface water at the Northern Gulf of Mexico, measured with a neuston (335 µm mesh size), varies between 0.05 and 0.184 pieces/m^2, while concentrations in the upper 15m of the water column, measured with a bongo (335 µm mesh size) varies between 0.048 and 0.082 pieces/m^2 (Tables 10 and 11). Concentrations at the seabed were between 1031 ± 5088 and 18046 ± 5088 pieces/m^2, thus are a factor 2.1E4 ± 1E5 to 9.8E5 ± 2.8E4 higher compared to the surface waters and 1.3E4 ± 6.2E4 to 3.8 ± 1.1E5. These factors are higher compared to the discrepancy between global measured and modelled concentrations in surface waters, which is E2. This emphasizes that river deltas are an important sink for microplastics.

An important sink for microplastics in the Gulf of Mexico might be the Mississippi Canyon, located at the east of our sample sites. Wei et al. (2012) documented a high abundance and a large variety of anthropogenic litter at this canyon, with the main abundance of (macro)plastic. Canyons has been shown to act as dumping sites for litter due to underwater currents and channeling effects (Galgani et al., 1996; Pham et al., 2014).

In general, fibers are the dominant type of microplastics reported (Mauro et al., 2017; Yu et al., 2018) at the surface water, water column and seabed. Fibers at beach sediments across the entire Gulf of Mexico were identified as PET (Yu et al. 2018). Based on this finding, fibers at the seabed would likely be partially identified as PET. Beach sediments on the east side of the Mississippi River have a dominance of hard plastics (Wessel et al., 2018). Polymer types are not always well reported in studies conducted in the Gulf of Mexico. Reported polymer types in beach sediments of Mobile Bay are PE, PP, PS, PA and polyester (Wessel et al., 2016) Besides the polyester, these findings are similar as observed polymer types at the sediments from the seabed in this study.

Based on comparing the microplastic concentrations from the seabed at this study to several beaches across the Gulf of Mexico, the surface waters and the upper 15 m water column close to the Mississippi river mouth, the seabed seems to be an important sink for microplastics. However, comparing these results should be done with care, due to the expression of microplastic concentration in different units, the use of extraction solutions with variable densities and variable mesh sizes (200-335 µm) and filter sizes (0.7-1 µm) (Tables 10 and 11). Water column data of microplastic concentrations at intermediate water depths is lacking. Studies should be performed throughout the water column to test the hypothesis of Kooi et al. (2017) that intermediate water depths are likely a potential sink for microplastic.

4.5 River deltas compared

Marine sediments at the Dutch river delta has been studied at 11 locations at the North Sea and two locations at the Rhine Estuary. Concentrations at the North Sea vary between 100 and 720 pieces/kg dw (265 and 1908 pieces/m^2) and at the Rhine Estuary between 3010-3600 pieces/kg dw (8003 and 9540 pieces/m^2). The average concentrations are 438 ± 139 pieces/kg dw (1160 ± 421 pieces/m^2) and 3305 ± 417 pieces/kg dw (8785 ± 1113 pieces/m^2) respectively.

Surface waters and the water column has not been studied at the North Sea. The model study of Eriksen et al. (2014) estimated microplastic concentrations at surface waters to be in the order of magnitude of E-2 pieces/m^2. Based on this, the microplastic concentrations at the seabed is 4 to 5 orders of magnitude higher compared to surface waters. This corresponds to our findings. Both the findings of Leslie et al. (2017) and this study support the hypothesis that marine sediments are an important sink for microplastics at the ocean.

Table 12. Study performed to microplastics performed at the Dutch River Delta, compared to this study and a model study. Given are the location, type of samples taken, surface area and depth of the samples, and the used methods. FTIR = Fourier Transform Infrared spectroscopy.

Study	Location	Sample type	Sample area and depth	Method
This study	Mississippi River delta. A transect from the river mouth to offshore	Marine sediments	79 cm^2, 5 cm depth	Density separation ZnCl2 (1.5 g/cm^2). Visual analysis, Raman-spectroscopy
Leslie et al., 2017	Dutch river delta	Marine sediments	Top 10 cm	Van Veen Grab, Density seperation NaCl (1.2 g/cm^3) Visual analysis, FTIR
		Estuarine sediments	Top 10 cm	Van Veen Grab, Density seperation NaCl (1.2 g/cm^3) Visual analysis, FTIR
Eriksen et al., 2014	North Sea	Surface waters	-	model

*Table 13. Study performed to microplastics performed at the Dutch River Delta, compared to this study and a model study, the found concentrations, the size and type of microplastics (H= hard plastics, B = microplastics, **Fb**= fibers) and the polymer type (HDPE = high-density polyethylene, LDPE = low-density polyethylene, PP = polypropylene, PS = polystyrene, PA = polyamide). Concentrations are given in both pieces/kg dw and pieces/m^2. Values in black are as reported in the paper, values in red are the converted values according equation 2.*

Study	**Concentration (unit)**	**Size (µm)**		**Types of plastics**	**Polymer types**
This study	303 ± 960 – 2705 ± 960 pieces/kg dw 1031 ± 5088 – 18046 ± 5088 pieces/m^2	180 - 643		**Fb**, H, B	HDPE, LDPE, PP, PS, PVC, PA, unknown
Leslie et al., 2017	100 – 720 pieces/kg dw, an average of 438 ± 159 pieces/kg dw 265- 1908 pieces/m^2, an average of 1160 ± 421 pieces/m^2	54% <300	46 % >300	**FB,** H, B	Not specified
	3020 – 3600 pieces/kg dw, an average of 3305 ± 417 pieces/kg dw 8003 – 9540 pieces/m^2, an average of 8758 ± 1113 pieces/m^2.	20% <300	80% > 300	**FB,** H, B	Not specified
Eriksen et al., 2014	In the order of E-2 pieces/m^2.	< 4.75 mm		H **(Fb?)**	-

4.6 Comparability of the microplastic distribution

Comparing reported concentrations of microplastics should be done with care, because of several reasons. First of all, the concentrations are expressed in different units from pieces per surface area or pieces per volume or sediment weight. Special attention should be given to pieces/surface area because sampled sediment depths varying from 1 cm to 10 cm have been used (Tables 8, 10 and 12). In addition, it has not always been made clear if the concentration is calculated for the entire depth-interval or for the top 1 cm of sediment or surface water. Second, varying mesh sizes have been used for water sampling and variable filters sizes for extraction of microplastics from the sediment (Tables 9, 11, 13). This can have a significant effect on the measured microplastic concentration, as the number of microplastics exponential increase with decreasing size (Mauro et al., 2017). Bergman et al. (2017) reported that 80% of the found microplastics were smaller than 25 µm.

Third, the sedimentation rate is highly variable per location and therefore similar sediment depth

intervals may represent different time intervals. As a result, the top 1 cm in deep-sea sediments could contain all microplastics that have ever been deposited due to sedimentation rates of mm/kyr. While this is not the case for the top 10 cm in coastal areas due to sedimentation rates of cm/yr. In general, sedimentation rates are not reported in microplastic studies. Another factor affecting the comparability of reported MP concentrations are the bioturbation intensity and mixing depth in soft marine sediments (Tael et al., 2008). Bioturbation could transport deposited microplastics deeper into the sediment and might cause a loss of initial deposited MP in the analyzed depth interval. Both the mixing depth and mixing intensity is site dependent. Mixing depth varying from 0 to 50 mm, and the mixing intensity from 0 to 380 cm^2/yr (Tael et al., 2008). As a result of inconsistent reported microplastic concentrations, variable sample and identification techniques, variable sedimentation rates and the effect of bioturbation, concentrations at different locations should be compared with caution.

We suggest that, in future studies, the depth interval over which a concentration has been calculated should be mentioned explicitly, as well as the sedimentation rate at the particular location. Moreover, it is suggested to express the microplastic concentration in standardized units to make findings of different studies comparable. We suggest to use pieces per dry weight for sediments, because a) this unit encloses a volume, b) concentrations between studies can be directly compared, c) it can easily be converted to pieces/m^2 when comparison to surface water are desirable, d) with a known sedimentation rate the time-interval of the sampled depth interval can be calculated and e) the porosity is excluded.

5. Conclusion

Microplastics are present along the entire depth transect in sediments of the Gulf of Mexico, from the Mississippi River mouth into the deep sea. Fibers have been found to be the most dominant type of microplastics. Other observed microplastic types are hard plastics and microbeads of both buoyant and non-buoyant polymer types. The microplastic composition is different per sampling station. The distribution of microplastics at the river delta is likely controlled by the combination of the input by varying sources, surface currents, primary productivity and the bathymetry of the seafloor. The Mississippi River is a main source of microplastic.

The comparison of microplastic concentrations in beach-, coastal-, and seabed sediments, surface waters and the water column, demonstrate that seabed sediments have the highest concentration of microplastics. Therefore, it can be concluded that the seabed is an important sink for microplastics at the MRD. Although, this conclusion is based on the minor data that was available. To test our findings on the minor available data, we suggest that the Mississippi delta should be studied more, on the microplastic concentration in the seabed, beach sediments, surface waters and the water column. In addition, similar studies in river deltas worldwide should be performed to improve our understanding of the fate of riverine input of plastic debris. Finally, these findings can be used to improve models of ocean (micro)plastic distribution. These are currently lacking the transfer of (micro)plastics from the surface waters to the seabed.

Our method is not suitable to give an exact amount of fiber concentration due to contamination and the lack of spectral analysis, but it gives a first estimation of the order of magnitude. Minor contamination is observed of hard plastics, degradation products from the SMI unit, but when it is found it can be controlled by blanks. Moreover, we experienced difficulties to compare different study sites as a result of the different use of units. Therefore, we call for standardized automated method strategies, to create more reliable data, where there is no loss of potential microplastic particles, no human bias and a reduced change for contamination.

References

Abidli, S., Antunes, J. C., Ferreira, J. L., Lahbib, Y., Sobral, P., & El Menif, N. T. (2018). Microplastics in sediments from the littoral zone of the north Tunisian coast (Mediterranean Sea). *Estuarine, Coastal and Shelf Science*, *205*, 1-9.

Alldredge, A. L., & Silver, M. W. (1988). Characteristics, dynamics and significance of marine snow. *Progress in oceanography*, *20*(1), 41-82.

Alomar, C., Estarellas, F., & Deudero, S. (2016). Microplastics in the Mediterranean Sea: deposition in coastal shallow sediments, spatial variation and preferential grain size. *Marine environmental research*, *115*, 1-10.

Andrady, A. L. (Ed.). (2003). *Plastics and the Environment*. John Wiley & Sons.

Andrady, A. L. (2011). Microplastics in the marine environment. *Marine pollution bulletin*, *62*(8), 1596-1605.

Andrady, A. L. (2015). Persistence of plastic litter in the oceans. In *Marine anthropogenic litter* (pp. 57-72). Springer, Cham.

Barnes, D. K., Galgani, F., Thompson, R. C., & Barlaz, M. (2009). Accumulation and fragmentation of plastic debris in global environments. *Philosophical Transactions of the Royal Society B: Biological Sciences*, *364*(1526), 1985-1998.

Bergmann, M., Wirzberger, V., Krumpen, T., Lorenz, C., Primpke, S., Tekman, M. B., & Gerdts, G. (2017). High quantities of microplastic in Arctic deep-sea sediments from the HAUSGARTEN observatory. *Environmental science & technology*, *51*(19), 11000-11010.

Bergmann, M., Lutz, B., Tekman, M. B., & Gutow, L. (2017). Citizen scientists reveal: Marine litter pollutes Arctic beaches and affects wild life. *Marine pollution bulletin*, *125*(1-2), 535-540.

Boerger, C. M., Lattin, G. L., Moore, S. L., & Moore, C. J. (2010). Plastic ingestion by planktivorous fishes in the North Pacific Central Gyre. *Marine pollution bulletin*, *60*(12), 2275-2278

BlueTech Research, (2014). BlueTech Chart of The Month Number Comparison: US Municipal Treatment Plants by Flow. Retrieved from: https://www.bluetechresearch.com/charts/bluetech-chart-month-number-comparison-us-municipal-treatment-plants-flow/

Blumenröder, J., Sechet, P., Kakkonen, J. E., & Hartl, M. G. J. (2017). Microplastic contamination of intertidal sediments of Scapa Flow, Orkney: a first assessment. *Marine pollution bulletin*, *124*(1), 112-120.

Browne, M. A., Dissanayake, A., Galloway, T. S., Lowe, D. M., & Thompson, R. C. (2008). Ingested microscopic plastic translocates to the circulatory system of the mussel, Mytilus edulis (L.). *Environmental science & technology*, *42*(13), 5026-5031.

Browne, M. A., Crump, P., Niven, S. J., Teuten, E., Tonkin, A., Galloway, T., & Thompson, R. (2011). Accumulation of microplastic on shorelines woldwide: sources and sinks. *Environmental science & technology*, *45*(21), 9175-9179.

Chen, Q., Reisser, J., Cunsolo, S., Kwadijk, C., Kotterman, M., Proietti, M., ... & Yin, D. (2017). Pollutants in plastics within the north Pacific subtropical gyre. *Environmental science & technology*, *52*(2), 446-456.

Choy, C. A., & Drazen, J. C. (2013). Plastic for dinner? Observations of frequent debris ingestion by pelagic predatory fishes from the central North Pacific. *Marine Ecology Progress Series*, *485*, 155-163.

Clark, J. R., Cole, M., Lindeque, P. K., Fileman, E., Blackford, J., Lewis, C., ... & Galloway, T. S. (2016). Marine microplastic debris: a targeted plan for understanding and quantifying interactions with marine life. *Frontiers in Ecology and the Environment*, *14*(6), 317-324.

Cole, M., Webb, H., Lindeque, P. K., Fileman, E. S., Halsband, C., & Galloway, T. S. (2014). Isolation of microplastics in biota-rich seawater samples and marine organisms. *Scientific reports*, *4*, 4528.

Coppock, R. L., Cole, M., Lindeque, P. K., Queirós, A. M., & Galloway, T. S. (2017). A small-scale, portable method for extracting microplastics from marine sediments. *Environmental Pollution*, *230*, 829-837.

Cózar, A., Echevarría, F., González-Gordillo, J. I., Irigoien, X., Úbeda, B., Hernández-León, S., ... & Fernández-de-Puelles, M. L. (2014). Plastic debris in the open ocean. *Proceedings of the National Academy of Sciences*, *111*(28), 10239-10244.

Crichton, E. M., Noël, M., Gies, E. A., & Ross, P. S. (2017). A novel, density-independent and FTIR-compatible approach for the rapid extraction of microplastics from aquatic sediments. *Analytical Methods*, *9*(9), 1419-1428.

Dantas, D. V., Barletta, M., & Da Costa, M. F. (2012). The seasonal and spatial patterns of ingestion of polyfilament nylon fragments by estuarine drums (Sciaenidae). *Environmental Science and Pollution Research*, *19*(2), 600-606.

Dobretsov, S. (2010). Marine biofilms. *Biofouling*, 123-136.

Dris, R., Gasperi, J., Saad, M., Mirande, C., & Tassin, B. (2016). Synthetic fibers in atmospheric fallout: a source of microplastics in the environment?. *Marine pollution bulletin*, *104*(1-2), 290-293.

EPA, United State Environmental Protection Agency (2018, December 2). The Mississippi/Atchafalaya River Basin (MARB) Retrieved from: https://www.epa.gov/ms-htf/mississippiatchafalaya-river-basin-marb

Eriksen, M., Maximenko, N., Thiel, M., Cummins, A., Lattin, G., Wilson, S., ... & Rifman, S. (2013). Plastic pollution in the South Pacific subtropical gyre. *Marine pollution bulletin*, *68*(1-2), 71-76.

Eriksen, M., Lebreton, L. C., Carson, H. S., Thiel, M., Moore, C. J., Borerro, J. C., ... & Reisser, J. (2014). Plastic pollution in the world's oceans: more than 5 trillion plastic pieces weighing over 250,000 tons afloat at sea. *PloS one*, *9*(12), e111913.

Fischer, V., Elsner, N. O., Brenke, N., Schwabe, E., & Brandt, A. (2015). Plastic pollution of the Kuril–Kamchatka Trench area (NW pacific). *Deep Sea Research Part II: Topical Studies in Oceanography*, *111*, 399-405.

Fischer, M., & Scholz-Böttcher, B. M. (2017). Simultaneous trace identification and quantification of common types of microplastics in environmental samples by pyrolysis-gas chromatography–mass spectrometry. *Environmental science & technology*, *51*(9), 5052-5060.

Fischer, E.K., Mordecai, P.J., Pfeiffer, F. (2018). Evaluation of various digestion protocols within microplastic sample processing concerning their efficiency of organic matter destruction and the resistance of different polymers. *Preleminary results showed at MICRO-conference 2018.*

Foekema, E. M., De Gruijter, C., Mergia, M. T., van Franeker, J. A., Murk, A. J., & Koelmans, A. A. (2013). Plastic in north sea fish. *Environmental science & technology*, *47*(15), 8818-8824.

Graham, E. R., & Thompson, J. T. (2009). Deposit-and suspension-feeding sea cucumbers (Echinodermata) ingest plastic fragments. *Journal of Experimental Marine Biology and Ecology*, *368*(1), 22-29.

Galloway, T. S., Cole, M., & Lewis, C. (2017). Interactions of microplastic debris throughout the marine ecosystem. *Nature ecology & evolution*, *1*(5), 0116.

Galgani, F., A. Souplet, and Y. Cadiou. "Accumulation of debris on the deep sea floor off the French Mediterranean coast." *Marine Ecology Progress Series* 142 (1996): 225-234.

Galgani, F., A., Hanke, G., Maes, T. (2015). Global Distribution, Composition and Abundance of Marine Litter. In *Marine anthropogenic litter* (pp. 29-56). Springer, Cham.

Green, D. S., Boots, B., Blockley, D. J., Rocha, C., & Thompson, R. (2015). Impacts of discarded plastic bags on marine assemblages and ecosystem functioning. *Environmental science & technology*, *49*(9), 5380-5389.

Hanke, G., Galgani, F., Werner, S., Oosterbaan, L., Nilsson, P., Fleet, D., et al. (2013). MSFD GES technical subgroup on marine litter. Guidance on monitoring of marine litter in European Seas. Luxembourg: Joint Research Centre–Institute for Environment and Sustainability, Publications Office of the European Union.

Hidalgo-Ruz, V., Gutow, L., Thompson, R. C., & Thiel, M. (2012). Microplastics in the marine environment: a review of the methods used for identification and quantification. *Environmental science & technology*, *46*(6), 3060-3075.

Hidalgo-Ruz, V., Honorato-Zimmer, D., Gatta-Rosemary, M., Nuñez, P., Hinojosa, I. A., & Thiel, M. (2018). Spatio-temporal variation of anthropogenic marine debris on Chilean beaches. *Marine pollution bulletin*, *126*, 516-524.

Hurley, R.R., Lusher, A.L., Olsen, M., Nizzetto, L. (unpublished). Validation of a Method for extraction microplastics from complex, organic-rich, environmental matrices. Environmental Science and Technolgoy.

Imhof, H. K., Schmid, J., Niessner, R., Ivleva, N. P., & Laforsch, C. (2012). A novel, highly efficient method for the separation and quantification of plastic particles in sediments of aquatic environments. *Limnology and oceanography: methods*, *10*(7), 524-537.

Jambeck, J. R., Geyer, R., Wilcox, C., Siegler, T. R., Perryman, M., Andrady, A., ... & Law, K. L. (2015). Plastic waste inputs from land into the ocean. *Science*, *347*(6223), 768-771.

Jenkins, C. (2018). Sediment Accumulation Rates For the Mississippi Delta Region: a Time-interval Synthesis. *Journal of Sedimentary Research*, *88*(2), 301-309.

Khatmullina, L., & Isachenko, I. (2017). Settling velocity of microplastic particles of regular shapes. *Marine pollution bulletin*, *114*(2), 871-880

Koelmans, A. A., Besseling, E., & Shim, W. J. (2015). Nanoplastics in the aquatic environment. Critical review. In *Marine anthropogenic litter* (pp. 325-340). Springer, Cham.

Kooi, M., Nes, E. H. V., Scheffer, M., & Koelmans, A. A. (2017). Ups and downs in the ocean: effects of biofouling on vertical transport of microplastics. *Environmental Science & Technology*, *51*(14), 7963-7971.

Kukulka, T., Proskurowski, G., Morét-Ferguson, S., Meyer, D. W., & Law, K. L. (2012). The effect of wind mixing on the vertical distribution of buoyant plastic debris. *Geophysical Research Letters*, *39*(7).

Kusui, T., & Noda, M. (2003). International survey on the distribution of stranded and buried litter on beaches along the Sea of Japan. *Marine Pollution Bulletin*, *47*(1-6), 175-179.

La Daana, K. Kanhai, Katarina Gårdfeldt, Olga Lyashevska, Martin Hassellöv, Richard C. Thompson, and Ian O'Connor. "Microplastics in sub-surface waters of the Arctic Central Basin." *Marine pollution bulletin* 130 (2018): 8-18.

Laist, D. W. (1997). Impacts of marine debris: entanglement of marine life in marine debris including a comprehensive list of species with entanglement and ingestion records. In *Marine Debris* (pp. 99-139). Springer, New York, NY.

Lavers, J. L., & Bond, A. L. (2017). Exceptional and rapid accumulation of anthropogenic debris on one of the world's most remote and pristine islands. *Proceedings of the National Academy of Sciences*, *114*(23), 6052-6055.

Law, K. L., Morét-Ferguson, S., Maximenko, N. A., Proskurowski, G., Peacock, E. E., Hafner, J., & Reddy, C. M. (2010). Plastic accumulation in the North Atlantic subtropical gyre. *Science*, *329*(5996), 1185-1188.

Law, K. L. (2017). Plastics in the marine environment. *Annual review of marine science*, *9*, 205-229.

Lebreton, L., Andrady, A. (unpublished). Future scenarios of global plastic waste production and disposal.

Lebreton, L. C., Van der Zwet, J., Damsteeg, J. W., Slat, B., Andrady, A., & Reisser, J. (2017). River plastic emissions to the world's oceans. *Nature communications*, *8*, 15611.

Lebreton, L., Slat, B., Ferrari, F., Sainte-Rose, B., Aitken, J., Marthouse, R., ... & Noble, K. (2018). Evidence that the Great Pacific Garbage Patch is rapidly accumulating plastic. *Scientific reports*, *8*(1), 4666.

Lecke-Mitchell, K.M., Mullin, K. (1997). Floating Marine Debris in the US Gulf of Mexico. *Marine Pollution Bulletin 34(9),* pp. 702-705.

Lenz, R., Enders, K., Stedmon, C. A., Mackenzie, D. M., & Nielsen, T. G. (2015). A critical assessment of visual identification of marine microplastic using Raman spectroscopy for analysis improvement. *Marine pollution bulletin*, *100*(1), 82-91.

Liebezeit, G., & Dubaish, F. (2012). Microplastics in beaches of the East Frisian islands Spiekeroog and Kachelotplate. *Bulletin of Environmental Contamination and Toxicology*, *89*(1), 213-217.

Löder, M. G., & Gerdts, G. (2015). Methodology used for the detection and identification of microplastics—A critical appraisal. In *Marine anthropogenic litter* (pp. 201-227). Springer, Cham.

Long, S. L., Gahan, C. G., & Joyce, S. A. (2017). Interactions between gut bacteria and bile in health and disease. *Molecular aspects of medicine*, *56*, 54-65. de Madron, X. D., Zervakis, V., Theocharis, A., & Georgopoulos, D. (2005). Comments on "Cascades of dense water around the world ocean". *Progress in Oceanography*, *64*(1), 83-90.

Maes, T., Van der Meulen, M. D., Devriese, L. I., Leslie, H. A., Huvet, A., Frère, L., ... & Vethaak, A. D. (2017). Microplastics baseline surveys at the water surface and in sediments of the North-East Atlantic. *Frontiers in Marine Science*, *4*, 135.

Mato, Y., Isobe, T., Takada, H., Kanehiro, H., Ohtake, C., & Kaminuma, T. (2001). Plastic resin pellets as a transport medium for toxic chemicals in the marine environment. *Environmental science & technology*, *35*(2), 318-324.

Martins, J., & Sobral, P. (2011). Plastic marine debris on the Portuguese coastline: a matter of size?. *Marine pollution bulletin*, *62*(12), 2649-2653.

McDermid, K. J., & McMullen, T. L. (2004). Quantitative analysis of small-plastic debris on beaches in the Hawaiian archipelago. *Marine pollution bulletin*, *48*(7-8), 790-794.

Murray, F., & Cowie, P. R. (2011). Plastic contamination in the decapod crustacean Nephrops norvegicus (Linnaeus, 1758). *Marine pollution bulletin*, *62*(6), 1207-1217.

Michel, R. L. (1992). Residence times in river basins as determined by analysis of long-term tritium records. *Journal of Hydrology*, *130*(1-4), 367-378.

Nichols, G. (2009). *Sedimentology and stratigraphy* (2nd ed.). Chichester, UK ; Hoboken, NJ: Wiley-Blackwell.

Nor, N. H. M., & Obbard, J. P. (2014). Microplastics in Singapore's coastal mangrove ecosystems. *Marine pollution bulletin*, *79*(1-2), 278-283.

Nor, N. H. M., & Obbard, J. P. (2014). Microplastics in Singapore's coastal mangrove ecosystems. *Marine pollution bulletin*, *79*(1-2), 278-283.

Norén, F., Norén, K., & Magnusson, K. (2014). Marint mikroskopiskt skräp. Undersökning längs svenska västkusten. In *Tech. rep*.

NPS, 2017. Mississippi river Facts. Retrieved from: https://www.nps.gov/miss/riverfacts.htm (jan,

2018)

Nuelle, M. T., Dekiff, J. H., Remy, D., & Fries, E. (2014). A new analytical approach for monitoring microplastics in marine sediments. *Environmental Pollution*, *184*, 161-169.

Obbard, R. W., Sadri, S., Wong, Y. Q., Khitun, A. A., Baker, I., & Thompson, R. C. (2014). Global warming releases microplastic legacy frozen in Arctic Sea ice. *Earth's Future*, *2*(6), 315-320.

Ocean currents. (2018) Retrieved from: https://www.noaa.gov/resource-collections/ocean-currents

Oey, L. Y. (2008). Loop Current and deep eddies. *Journal of Physical Oceanography*, *38*(7), 1426-1449.

Peeken, I., Primpke, S., Beyer, B., Gütermann, J., Katlein, C., Krumpen, T., ... & Gerdts, G. (2018). Arctic sea ice is an important temporal sink and means of transport for microplastic. *Nature communications*, *9*(1), 1505.

Peng, X., Chen, M., Chen, S., Dasgupta, S., Xu, H., Ta, K., ... & Bai, S. (2018). Microplastics contaminate the deepest part of the world's ocean. *GEOCHEMICAL PERSPECTIVES LETTERS*, *9*, 1-5.

Pham, C. K., Ramirez-Llodra, E., Alt, C. H., Amaro, T., Bergmann, M., Canals, M., ... & Huvenne, V. A. (2014). Marine litter distribution and density in European seas, from the shelves to deep basins. *PloS one*, *9*(4), e95839.

Plastic Europe (2017). Plastics-the Facts 2017, An analysis of European plastics production, demand and waste data. Available from: www.plasticseurope.org

Porter, A., Lyons, B. P., Galloway, T. S., & Lewis, C. N. (2018). The role of marine snows in microplastic fate and bioavailability. *Environmental science & technology*.

Primpke, S., Lorenz, C., Rascher-Friesenhausen, R., & Gerdts, G. (2017). An automated approach for microplastics analysis using focal plane array (FPA) FTIR microscopy and image analysis. *Analytical Methods*, *9*(9), 1499-1511.

Railkin, A. I. (2003). *Marine biofouling: colonization processes and defenses*. CRC press.

Reisser, J., Shaw, J., Wilcox, C., Hardesty, B. D., Proietti, M., Thums, M., & Pattiaratchi, C. (2013). Marine plastic pollution in waters around Australia: characteristics, concentrations, and pathways. *PloS one*, *8*(11), e80466.

Renner, G., Schmidt, T. C., & Schram, J. (2017). A new chemometric approach for automatic identification of microplastics from environmental compartments based on FT-IR spectroscopy. *Analytical chemistry*, *89*(22), 12045-12053.

Richard, C.E. (2016) The Atchafalaya River Basin: History and Ecology of an American Wetland, The AAG Review of Books, 4:2, 69-71

Rivas, D., Badan, A., & Ochoa, J. (2005). The ventilation of the deep Gulf of Mexico. *Journal of physical oceanography*, *35*(10), 1763-1781.

Rochman, C. M., Hoh, E., Kurobe, T., & Teh, S. J. (2013). Ingested plastic transfers hazardous chemicals to fish and induces hepatic stress. *Scientific reports*, *3*, 3263.

Ryan, P. G. (1987). The incidence and characteristics of plastic particles ingested by seabirds. *Marine Environmental Research*, *23*(3), 175-206.

Savoca, M. S., Tyson, C. W., McGill, M., & Slager, C. J. (2017). Odours from marine plastic debris induce food search behaviours in a forage fish. *Proceedings of the Royal Society B: Biological Sciences*, *284*(1860), 20171000.

Schmidt, C., Krauth, T., & Wagner, S. (2017). Export of plastic debris by rivers into the sea. *Environmental science & technology*, *51*(21), 12246-12253.

SeaWiFs-entire mission composite 1997-2010. Retrieved from: https://svs.gsfc.nasa.gov/30801

Shim, W. J., & Thomposon, R. C. (2015). Microplastics in the ocean. *Archives of environmental contamination and toxicology*, *69*(3), 265-268.

Silva, A. B., Bastos, A. S., Justino, C. I., da Costa, J. P., Duarte, A. C., & Rocha-Santos, T. A. (2018). Microplastics in the environment: Challenges in analytical chemistry-A review. *Analytica chimica acta*.

Syed, T. H., Famiglietti, J. S., Chen, J., Rodell, M., Seneviratne, S. I., Viterbo, P., & Wilson, C. R. (2005). Total basin discharge for the Amazon and Mississippi River basins from GRACE and a land-atmosphere water balance. *Geophysical Research Letters*, *32*(24).

Teal, L. R., Bulling, M. T., Parker, E. R., & Solan, M. (2008). Global patterns of bioturbation intensity and mixed depth of marine soft sediments. *Aquatic Biology*, *2*(3), 207-218.

Tekman, M. B., Krumpen, T., & Bergmann, M. (2017). Marine litter on deep Arctic seafloor continues to increase and spreads to the North at the HAUSGARTEN observatory. *Deep sea research part I: oceanographic research papers*, *120*, 88-99.

Teuten, E. L., Saquing, J. M., Knappe, D. R., Barlaz, M. A., Jonsson, S., Björn, A., ... & Ochi, D. (2009). Transport and release of chemicals from plastics to the environment and to wildlife. *Philosophical Transactions of the Royal Society B: Biological Sciences*, *364*(1526), 2027-2045.

TOXNET. (dec, 2018). Retrieved from: https://toxnet.nlm.nih.gov/cgi-bin/sis/search/a?dbs+hsdb:@term+@DOCNO+1050

Tubau, X., Canals, M., Lastras, G., Rayo, X., Rivera, J., & Amblas, D. (2015). Marine litter on the floor of deep submarine canyons of the Northwestern Mediterranean Sea: the role of hydrodynamic processes. *Progress in Oceanography*, *134*, 379-403.

Turra, A., Manzano, A. B., Dias, R. J. S., Mahiques, M. M., Barbosa, L., Balthazar-Silva, D., & Moreira, F. T. (2014). Three-dimensional distribution of plastic pellets in sandy beaches: shifting paradigms. *Scientific reports*, *4*, 4435.

Turner, A., & Holmes, L. (2011). Occurrence, distribution and characteristics of beached plastic production pellets on the island of Malta (central Mediterranean). *Marine Pollution Bulletin*, *62*(2), 377-381.

US Census Bureau. (2016). Annual estimates of the resident population by sex, age, race, and Hispanic origin for the United States and states: April 1, 2010 to July 1, 2014.

Van Cauwenberghe, Lisbeth, et al. "Microplastic pollution in deep-sea sediments." *Environmental Pollution* 182 (2013): 495-499.

Van Helmond (2018). Data sediment porosity Northern Gulf of Mexico (NICO 2018). *Geochemistry group, Utrecht University*

Van Sebille, E., Wilcox, C., Lebreton, L., Maximenko, N., Hardesty, B. D., Van Franeker, J. A., ... & Law, K. L. (2015). A global inventory of small floating plastic debris. *Environmental Research Letters*, *10*(12), 124006.

Van der Wal, M., van der Meulen, M., Tweehuijsen, G., Peterlin, M., Palatinus, A., & Kovač Viršek, M. (2015). SFRA0025: Identification and Assessment of Riverine Input of (Marine) Litter.

Van Zummeren, R. (2019). Iron and manganese dynamics in the northeren Gulf of Mexico. *MSc thesis, UU*

Veiga, J. M., Fleet, D., Kinsey, S., Nilsson, P., Vlachogianni, T., Werner, S., ... & Sobral, P. (2016). Identifying Sources of Marine Litter. MSFD GES TG Marine Litter Thematic Report. In *JRC Technical Report*.

Vermaire, J. C., Pomeroy, C., Herczegh, S. M., Haggart, O., & Murphy, M. (2017). Microplastic abundance and distribution in the open water and sediment of the Ottawa River, Canada, and its tributaries. *Facets*, *2*(1), 301-314.

Vianello, A., Boldrin, A., Guerriero, P., Moschino, V., Rella, R., Sturaro, A., & Da Ros, L. (2013). Microplastic particles in sediments of Lagoon of Venice, Italy: First observations on occurrence, spatial patterns and identification. *Estuarine, Coastal and Shelf Science*, *130*, 54-61.

Walker, N. D., Pilley, C. T., Raghunathan, V. V., D'Sa, E. J., Leben, R. R., Hoffmann, N. G., ... & Turner, R. E. (2011). Impacts of Loop Current frontal cyclonic eddies and wind forcing on the 2010 Gulf of Mexico oil spill. *Monitoring and Modeling the Deepwater Horizon Oil Spill: A Record-Breaking Enterprise, Geophys. Monogr. Ser*, *195*, 103-116.

Wei, C. L., Rowe, G. T., Nunnally, C. C., & Wicksten, M. K. (2012). Anthropogenic "Litter" and macrophyte detritus in the deep Northern Gulf of Mexico. *Marine pollution bulletin*, *64*(5), 966-973.

Wessel, C. C., Lockridge, G. R., Battiste, D., & Cebrian, J. (2016). Abundance and characteristics of microplastics in beach sediments: insights into microplastic accumulation in northern Gulf of Mexico estuaries. *Marine pollution bulletin*, *109*(1), 178-183.

Woodall, L. C., Sanchez-Vidal, A., Canals, M., Paterson, G. L., Coppock, R., Sleight, V., ... & Thompson, R. C. (2014). The deep sea is a major sink for microplastic debris. *Royal Society open science*, *1*(4), 140317.

Wright, S. L., Thompson, R. C., & Galloway, T. S. (2013). The physical impacts of microplastics on marine organisms: a review. *Environmental pollution*, *178*, 483-492.

Yoshida, S., Hiraga, K., Takehana, T., Taniguchi, I., Yamaji, H., Maeda, Y., ... & Oda, K. (2016). A bacterium that degrades and assimilates poly (ethylene terephthalate). *Science*, *351*(6278), 1196-1199.

Yu, X., Ladewig, S., Bao, S., Toline, C. A., Whitmire, S., & Chow, A. T. (2018). Occurrence and distribution of microplastics at selected coastal sites along the southeastern United States. *Science of the Total Environment*, *613*, 298-305.

Zhou, Q., Zhang, H., Fu, C., Zhou, Y., Dai, Z., Li, Y., ... & Luo, Y. (2018). The distribution and morphology of microplastics in coastal soils adjacent to the Bohai Sea and the Yellow Sea. *Geoderma*, *322*, 201-208.

Zitko, V., & Hanlon, M. (1991). Another source of pollution by plastics: skin cleaners with plastic scrubbers. *Marine Pollution Bulletin*, *22*(1), 41-42.

Zobkov, M., & Esiukova, E. (2017). Microplastics in Baltic bottom sediments: quantification procedures and first results. Marine pollution bulletin, 114(2), 724-732.

Attachment I

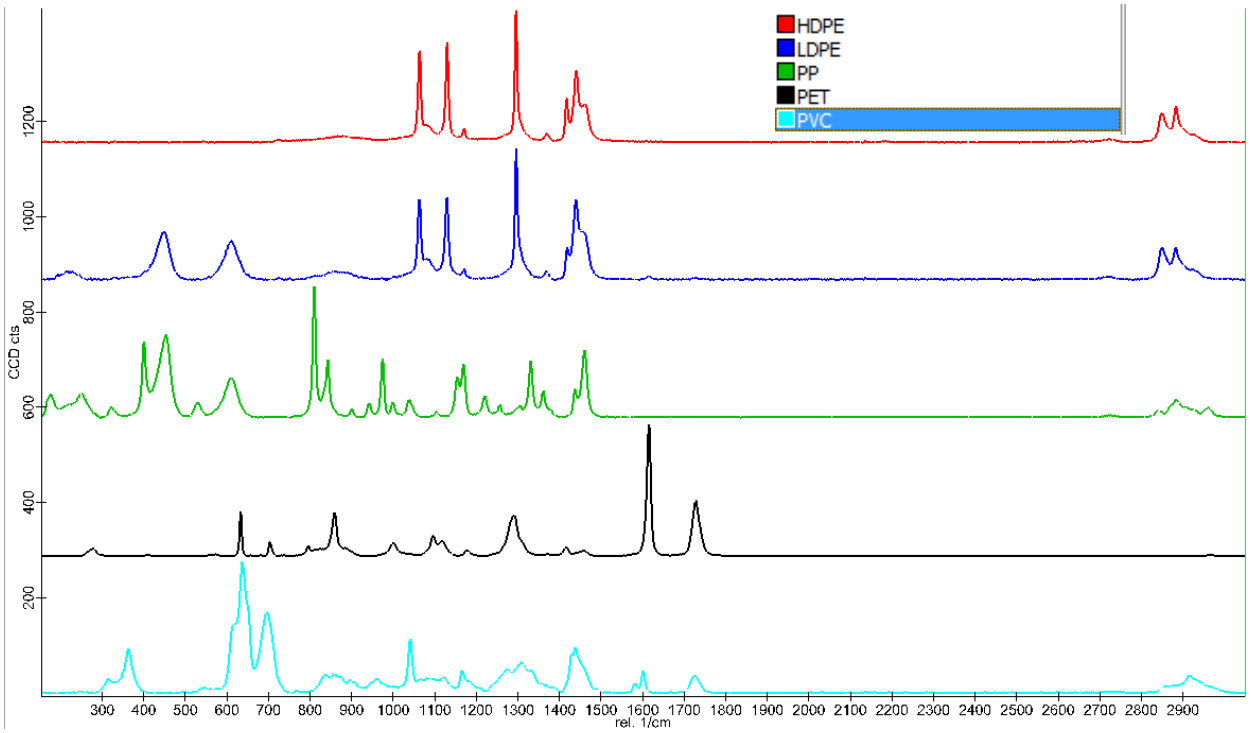

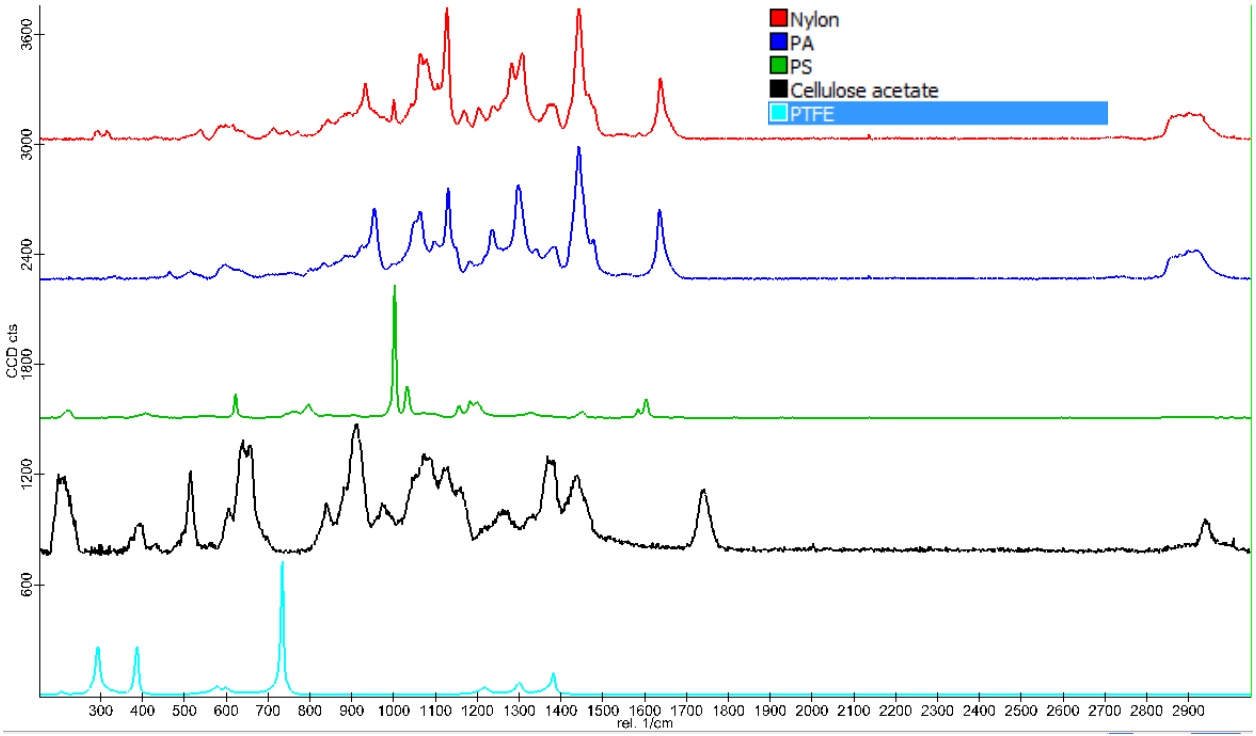

Attachment II